Engineering 53 (2025) 245–258

Contents lists available at ScienceDirect

Engineering

journal homepage: www.elsevier.com/locate/eng

Research
Antimicrobial Resistance—Article

Transmission of *tmexCD1-toprJ1*-Positive *Klebsiella pneumoniae* Across Multiple Ecological Niches: A Global Epidemiological and Genomic Analysis

Luchao Lv [a,#], Xun Gao [a,#], Chengzhen Wang [a,#], Guolong Gao [a], Jie Yang [a], Miao Wan [a], Zhongpeng Cai [a], Sheng Chen [d,e], Jing Wang [f], Chuying Liang [a], Chao Yue [a], Litao Lu [a], Zhiyong Zong [c,*], Jian-Hua Liu [a,b,*]

[a] *State Key Laboratory for Animal Disease Control and Prevention, Guangdong Laboratory for Lingnan Modern Agriculture, College of Veterinary Medicine, South China Agricultural University, Guangzhou 510642, China*
[b] *Key Laboratory of Zoonosis of Ministry of Agricultural and Rural Affairs, Guangzhou 510642, China*
[c] *Center of Infectious Diseases, West China Hospital of Sichuan University, Chengdu 610041, China*
[d] *State Key Lab of Chemical Biology and Drug Discovery and the Department of Food Science and Nutrition, The Hong Kong Polytechnic University, Hong Kong 999077, China*
[e] *Shenzhen Key Lab for Food Biological Safety Control, The Hong Kong Polytechnic University Shenzhen Research Institute, Shenzhen 518057, China*
[f] *Jiangsu Key Laboratory of Zoonosis, Jiangsu Co-Innovation Center for Prevention and Control of Important Animal Infectious Diseases and Zoonoses, Yangzhou University, Yangzhou 225009, China*

ARTICLE INFO

Article history:
Received 4 October 2024
Revised 3 March 2025
Accepted 13 March 2025
Available online 28 June 2025

Keywords:
tmexCD1-toprJ1
Tigecycline resistance
Klebsiella pneumoniae
Epidemiology

ABSTRACT

Tigecycline is one of the most critical drugs for treating Gram-negative bacterial infections; however, the emergence of the tigecycline resistance efflux pump TMexCD1-TOprJ1 poses a global health threat. The evolutionary relationships and epidemiological trends of *tmexCD1-toprJ1*-positive strains across various ecological niches remain largely unexplored. In this study, we employed whole-genome sequencing (WGS) of *tmexCD1-toprJ1*-positive bacteria from humans, food, animals, and the environment in China to assess the epidemiological and genomic features of these strains, analyzing both newly collected strains and data from the GenBank database. From 3 434 samples collected during 2019–2022, 145 *tmexCD1-toprJ1*-carrying strains (4.5%) were isolated. The majority of the *tmexCD1-toprJ1*-positive Enterobacterales exhibited resistance to nearly all antimicrobials, including colistin (42.13%). *tmexCD1-toprJ1* was predominantly identified in *Klebsiella pneumoniae* (*K. pneumoniae*) from chicken feces in China but was also detected in multiple ecological niches and other countries. Phylogenetic analysis revealed the clonal transmission of *tmexCD1-toprJ1*-positive ST37 *K. pneumoniae* across diverse ecological niches as well as the international spread of the ST15 *K. pneumoniae* clone-producing TMexCD1-TOprJ1. *tmexCD1-toprJ1* is mainly carried by *Klebsiella* spp. specific narrow host range plasmids, which may limit the spread of *tmexCD1-toprJ1* across different bacterial species. Notably, due to the fitness cost posed by *tmexCD1-toprJ1*, the occurrence of *tmexCD1-toprJ1*-positive Enterobacterales in both food animals and humans in China has declined significantly following the withdrawal of antibiotics as growth promoters in food animals in China since 2020. However, *tmexCD1-toprJ1* has been captured by broad-host-range plasmids and hypervirulent carbapenem-resistant *K. pneumoniae* ST11-KL64 strains in healthcare settings. The frequent use of tetracyclines in chicken farming likely contributes to the high detection rate of *tmexCD1-toprJ1*; therefore, to reduce the threat of *tmexCD1-toprJ1*-positive *K. pneumoniae*, continuous monitoring of *tmexCD1-toprJ1* across different ecological niches and strict enforcement of antimicrobial policies in animal husbandry, particularly in the poultry industry, are urgently required.

© 2025 THE AUTHORS. Published by Elsevier LTD on behalf of Chinese Academy of Engineering and Higher Education Press Limited Company. This is an open access article under the CC BY-NC-ND license (http://creativecommons.org/licenses/by-nc-nd/4.0/).

1. Introduction

An increase in antimicrobial resistance (AMR) poses a significant challenge to global public health. The emerging resistance to carbapenems is particularly concerning because these agents are

* Corresponding authors.
E-mail addresses: zongzhiy@scu.edu.cn (Z. Zong), jhliu21@163.com (J.-H. Liu).
# These authors contributed equally to this work.

https://doi.org/10.1016/j.eng.2025.03.038
2095-8099/© 2025 THE AUTHORS. Published by Elsevier LTD on behalf of Chinese Academy of Engineering and Higher Education Press Limited Company.
This is an open access article under the CC BY-NC-ND license (http://creativecommons.org/licenses/by-nc-nd/4.0/).

frequently considered the last line of effective therapy for infections caused by multidrug-resistant (MDR) Gram-negative bacteria. Due to a lack of effective treatment options, carbapenem-resistant Enterobacterales (CREs) have been classified as critical pathogens by the World Health Organization (WHO) [1]. Carbapenem-resistant *Klebsiella pneumoniae* (*K. pneumoniae*, CRKP) is the most frequently occurring CRE, and it significantly contributes to the global disease burden [2,3]. The pooled mortality rate associated with CRKP infections ranges from 24.2% to 33% [4,5]. In Europe alone, extended-spectrum beta-lactamases (ESBLs) and CRKP account for over 90 000 infections and over 7 000 deaths annually [3]. In China, the prevalence of carbapenem resistance in *K. pneumoniae* rose from 2.9% in 2005 to 26.0% in 2023 (China Antimicrobial Surveillance Network, CHINET), leading to untreatable nosocomial infections with mortality risks as high as 55.8% [6]. Consequently, treating *K. pneumoniae* infections with antimicrobial agents is becoming increasingly difficult, and the optimal therapeutic strategies remain unclear. Colistin and tigecycline are currently among the few antibiotics available for critically ill patients with CRKP infections [7–9]. However, the recent discovery of the plasmid-mediated colistin resistance gene *mcr-1* poses a significant threat to the clinical utility of colistin for treating these infections, leaving tigecycline as one of the only remaining treatment options.

Tigecycline, the first drug in the glycylcycline class of antibiotics, is classified as a critically important antimicrobial and reserve drug on the WHO List of Medically Important Antimicrobials and the WHO AWaRe classification list [10,11]. Therefore, the emergence of tigecycline resistance is a growing concern. Prior to 2019, the mechanisms of tigecycline resistance in Gram-negative bacteria were primarily linked to the overexpression of chromosomal efflux systems, mutations in ribosomal binding sites, and *tet*(A) mutations [12–15]. However, recently, two novel plasmid-mediated mechanisms of tigecycline resistance have surfaced: tetracycline-degrading enzymes (Tet(X) variants) and the resistance-nodulation-cell division (RND) efflux system (TMexCD1-TOprJ1). These mechanisms were first identified in bacteria of animal origin, and they pose a significant threat to the efficacy of tigecycline against infections caused by *K. pneumoniae* [7,9,16]. Unlike Tet(X) variants, which hydrolyze only tetracycline and are common in *Escherichia coli* and *Acinetobacter* spp. [7,9,17], TMexCD1-TOprJ1 can confer resistance to all tetracyclines and several other critical antimicrobials, including quinolones, cephalosporins, and aminoglycosides, primarily within *K. pneumoniae* [16,18]. To date, six plasmid-borne *tmexCD-toprJ*-like gene clusters have been identified, with *tmexCD1-toprJ1* conferring the highest level of tigecycline resistance, increasing minimum inhibitory concentrations (MICs) by 16–32-fold. In contrast, the other clusters only increased the MICs by 4–8-fold [19–25].

Antimicrobial resistance gene (ARG) transmission occurs via clonal strains or mobile genetic elements between humans, animals, food, and the environment [26]. Once certain ARGs have emerged in animals or humans, they can spread to various ecological niches. Given the clinical importance of tigecycline and the health risks posed by *K. pneumoniae*, the emergence of TMexCD1-TOprJ1-producing *K. pneumoniae* in food animals has gained significant attention. Epidemiological data indicate that TMexCD1-TOprJ1 is primarily found in food animals, particularly in chicken farms in China, but it has also been detected in human, food, and environmental samples [16,27–32]. Therefore, understanding the transmission patterns of *tmexCD1-toprJ1* across ecosystems and the evolutionary characteristics of its transmission vectors is crucial. However, to date, no large-scale molecular epidemiological studies have been conducted on *tmexCD1-toprJ1*.

In this study, we conducted the first nationwide surveillance of *tmexCD1-toprJ1*-positive isolates from various ecological niches, including farm animals, environments, retail meat, and humans in China. In addition, we included whole-genome sequences of *tmexCD1-toprJ1*-positive strains from GenBank for analysis. Our findings revealed severe multidrug resistance among *tmexCD1-toprJ1*-positive bacteria, with evidence of clonal transmission in both humans and chickens, including international transmission. Further, we observed a significant decline in the prevalence of *tmexCD1-toprJ1* from 2018 to 2022, which correlates with the implementation of policies restricting the use of antimicrobials as growth promoters in food animals in China.

2. Materials and methods

2.1. Sample collection and bacterial isolation

From September 2019 to December 2022, 3 434 samples were collected from seven provinces (Fujian, Guangdong, Henan, Hunan, Shandong, Sichuan, and Zhejiang), two autonomous regions (Guangxi, Xinjiang), and one municipality (Shanghai) of China (Table S1 in Appendix A). The samples were recovered from chicken feces (n = 1261), slaughtered chicken feces (n = 419), duck feces (n = 255), swine feces (n = 819), retail chicken meat (n = 59), pork (n = 113), chicken farm environments (n = 128), other environments (farmers' markets, schools, or stations) (n = 180), goose feces (n = 60), and vegetables (n = 140) (Table S1). All of the tigecycline-nonsusceptible isolates were screened on MacConkey plates supplemented with 4 $mg{\cdot}L^{-1}$ tigecycline. *tmexCD1-toprJ1*-positive isolates were detected via polymerase chain reaction (PCR) and further confirmed through Sanger sequencing (Tsingke Biotechnology, China) with previously reported primers [16]. The bacterial species of the isolates were determined using Bruker MALDI Biotyper (Bruker Daltonik GmbH, Germany) and 16S ribosomal DNA (rDNA) sequencing.

In addition, six *tmexCD1-toprJ1*-positive *Klebsiella* spp. isolates of human origin were collected from West China Hospital in Sichuan, China. These clinical isolates were obtained from samples collected during routine care for patients with infections. Patients consented to the care provided by the hospital and its staff, which included sample collection for infection management. Further, 455 *tmexCD1-toprJ1*-carrying isolates, including two from humans, 376 from chicken feces, nine from chicken meat, 25 from farm environments, and 11 from pork, obtained in our prior study [16], were also included in this study. We collected 1180 pig fecal samples from 21 pig farms (Table S2 in Appendix A) and 1702 chicken fecal samples from 29 chicken farms (Table S3 in Appendix A) in China in 2022 in order to determine the colonization rate of *K. pneumoniae* in the intestines of chickens and swine. The samples were inoculated on MacConkey agar, and colonies with different morphologies were selected from the agar for strain identification using Bruker MALDI Biotyper (Bruker Daltonik GmbH).

2.2. Antimicrobial susceptibility testing

The MICs of 13 antimicrobials, namely, imipenem, ceftazidime, cefotaxime, cefoxitin, ciprofloxacin, tigecycline, doxycycline, tetracycline, colistin, florfenicol, amikacin, gentamicin, and sulfamethoxazole-trimethoprim, were determined using the agar dilution or broth microdilution method (for tigecycline and colistin), with *Escherichia coli* (*E. coli*) ATCC 25922 serving as the quality control, in accordance with the standards outlined in the Clinical and Laboratory Standards Institute (CLSI) document M100, 31st Edition [33]. The agar dilution method was performed as follows: first, intermediate (10×) antimicrobial agent solution was prepared, typically at 640–1280 times the breakpoint concentration (e.g., 2560–5120 $\mu g{\cdot}mL^{-1}$), by performing serial two-fold

dilutions; next, one part of the intermediate (10×) antimicrobial agent solution was combined with nine parts of molten agar (e.g., 2 mL of antimicrobial agent solution to 18 mL of molten Mueller–Hinton agar), before adding appropriate dilutions of the antimicrobial agent solution to the molten Mueller-Hinton agar and ensuring thorough mixing before pouring it into Petri dishes to form agar plates. For tigecycline and colistin, self-prepared 96-well microdilution plates were used for MIC determination. Briefly, 100-μL Mueller–Hinton broth (MH broth) was added to each well of a 96-well plate. The stock solution of antimicrobial agent (tigecycline or colistin) was added to the first well using a two-fold serial dilution method, ensuring an equal volume of stock solution and broth (e.g., 100 μL of MH broth and 100 μL of stock solution in the first well), before thoroughly mixing the contents of each well. The remaining dilutions were completed by transferring the necessary volumes using a pipette. Three replicates were performed for each antimicrobial agent. Every plate included a growth control (broth with *E. coli* ATCC 25922 but no antimicrobial agent) and a sterility control (broth alone). The CLSI breakpoints were used to interpret the susceptibility results for most antimicrobial agents, except for tigecycline, for which the European Committee on Antimicrobial Susceptibility Testing (EUCAST) breakpoint was applied.

2.3. Conjugation assay and plasmid stability

The transferability of *tmexCD1-toprJ1*-carrying plasmids was evaluated via conjugation using sodium azide-resistant *E. coli* J53 as recipient. The transfer frequencies were calculated as the number of transconjugants per recipient. A plasmid stability assay was performed as previously described [34]. In brief, a single clone of the *tmexCD1-toprJ1*-positive strain was grown in Luria-Bertani (LB) broth, followed by serial passage every day at a 1:1000 dilution in LB broth for 15 days. The plasmid stability of the passaged bacteria was tested every two days. The stability of the *tmexCD1-toprJ1*-bearing plasmids was evaluated by dividing the number of colonies positive for the *tmexCD1-toprJ1*-bearing plasmid by the total number of colonies growing on antibiotic-free plates.

In vitro competition experiments were conducted using *tmexCD1-toprJ1* transconjugants (*E. coli* J53 and *K. pneumoniae* AH58I) alongside their corresponding recipient strains [35]. The transconjugants and recipients were mixed at a 1:1 ratio, and every 24 h, the mixed bacterial culture was inoculated into 10 mL of fresh LB broth at a 1:100 ratio for a total of 96 h. At 24, 48, 72, and 96 h, 100 μL of the mixed bacterial culture was collected, serially diluted, and plated onto LB agar plates. After incubation for 16–20 h, PCR was used to amplify *tmexCD1-toprJ1* for colony counting. The relative fitness (RF) of the strains was calculated using the formula RF = ln (Nf,S1/Ni,S1)/ln (Nf,S2/Ni,S2), where Nf, S1 and Ni,S1 represent the colony counts of recipient strain S1 and *tmexCD1-toprJ1* transconjugant S2 at 0 and 96 h, respectively.

2.4. Whole-genome sequencing (WGS) and bioinformatics analysis

The genomic DNA of 271 *tmexCD1-toprJ1*-positive isolates (95 from this study, and 176 from prior studies [16]), including 206 from chickens, 19 from chicken farms, 11 from chicken meat, ten from humans, eight from duck feces, eight from pork, seven from other environments (farmer's market environments), one from a goose feces, and one from a vegetable, was sequenced using the Illumina NovaSeq 6000 platform (Illumina, USA). The trimmed sequence reads were assembled using SPAdes [36] (v3.15.2; parameters: --careful --phred-offset 33 --cov-cutoff auto -k 21,31,55,77,99,127). The 271 *tmexCD1-toprJ1*-positive bacteria were selected based on the principle that approximately one-third to one-half of the isolates collected from poultry farm environments and chicken feces were randomly selected for sequencing, while almost all of the isolates obtained from other sources were sequenced. Fifty-five representative isolates (selected based on isolation source, location, species, and multilocus sequence typing (MLST)) were chosen for long-read sequencing via Nanopore MinION R10 (Oxford Nanopore Technologies, UK) or the QNome-3841 platform (QitanTech, China) in order to reveal the genetic features of these isolates. Illumina short reads and nanopore long reads were combined to obtain hybrid assembly data using Unicycler [37] (v0.4.8; parameters: --keep 0; --mode conservative) under conservative mode for increased accuracy. The genome sequences were annotated using bakta v1.5.1 [38].

ARGs, virulence factors, and plasmid replicons were identified using the Resfinder, VFDB, and PlasmidFinder databases, respectively, via Abricate v0.9.8 (--min-id 99 --min-cov 50). The species, MLST, *wzi* allele, and O and K serotypes were identified using Kleobrate v2.1.0 [39]. Heavy metal resistance genes were identified using the AMRFinderPlus [40]. The *tmexCD1-toprJ1*-carrying plasmids were further compared and analyzed using the BLAST Ring Image Generator (BRIG). ISfinder, Gene Construction Kit v4.5 (Textco BioSoftware, Inc., USA), and Easyfig were used to analyze the MDR regions of plasmids and the genetic context of *tmexCD1-toprJ1* [41]. The correlation between plasmid replicon types and ARGs was determined using the Pearson's correlation coefficient. The Mantel test was used to assess the correlation between plasmid replicon types, AMRs, and *tmexCD1-toprJ1* genetic types. Pearson's correlation analysis and the Mantel test were performed and visualized using the "vegan" and "LinkET" packages in R v4.3.0 (R Foundation for Statistical Computing, Austria).

In addition, to compare the number of acquired ARGs in bla_{NDM}-positive and bla_{KPC}-positive *K. pneumoniae* with that in *tmexCD1-toprJ1*-positive *K. pneumoniae* strains, we performed a search in the National Database of Antibiotic Resistant Organisms (NDARO) using the keywords "AMR_genotypes: bla_{NDM}* AND taxgroup_name: *Klebsiella pneumoniae* AND epi_type: clinical" and "AMR_genotypes: bla_{KPC}* AND taxgroup_name: *Klebsiella pneumoniae* AND epi_type: clinical". A total of 5 597 bla_{NDM} and 15 534 bla_{KPC} genomic datasets were returned from the NDARO database.

2.5. Search for tmexCD1-toprJ1 in GenBank

We collected *tmexCD1-toprJ1*-containing genomic sequences from the NCBI GenBank database in several ways in order to investigate the global prevalence of *tmexCD1-toprJ1*. First, a BLASTn search of the nucleotide (NT) database was performed to obtain strain sequences containing *tmexC1* or *tmexD1* with ≥ 99% identity prior to January 1, 2024. Second, genome data from the NCBI Assembly database were downloaded (January 2024) with "Enterobacterales" annotation in GenBank. Next, *tmexCD1*-carrying genome data were collected by searching *tmexC1-tmexD1* nucleotide sequences with ≥ 99% identity via Abricate (--min-id 99 --min-cov 50). In addition, the NDARO was searched for *tmexCD1-toprJ1*-carrying strains. For all of the *tmexCD1-toprJ1*-containing sequences, basic information on the corresponding strains, including isolation sources, dates, and cities, was collected.

Further, we employed MLST software to retrieve the genomes of 960 ST37-type *K. pneumoniae* strains from the "Enterobacterales" dataset.

2.6. Phylogenetic analyses

Core genome single-nucleotide polymorphisms (SNPs) between different strains were analyzed using snippy 4.6.0 to determine the transmission routes of the *tmexCD1-toprJ1* gene cluster. A pairwise

SNP matrix was generated using snp-dists. Core-genome SNP-based neighbor-joining phylogenetic trees were constructed for *tmexCD1-toprJ1*-positive *K. pneumoniae* using Parsnp 1.5.3 [42]. Clustering of *tmexCD1-toprJ1*-positive *K. pneumoniae* was examined using hierarchical Bayesian analysis of population structure (hierBAPS) [43]. Interactive tree of life (iTOL) was used to manage and visualize the trees [44]. A minimum spanning tree of all of the sequence types (STs) was constructed using BioNumerics software v7.6 (Applied Maths, Belgium).

3. Results

3.1. Prevalence and characterization of tmexCD1-toprJ1-positive isolates

From November 2019 to December 2022, a total of 145 (4.2%) *tmexCD1-toprJ1*-positive isolates that were obtained from 3434 samples collected in China (Fig. 1). The highest isolation rates were observed in chicken farm environments (14.1%, *n* = 18) and chicken feces (7.0%, *n* = 88), followed by chicken meat samples (6.8%, *n* = 4), duck feces (5.1%, *n* = 13), fecal samples from slaughtered chickens (3.8%, *n* = 16), other environmental samples (1.7%, *n* = 3), goose feces (1.7%, *n* = 1), pork samples (0.9%, *n* = 1), and vegetable samples (0.7%, *n* = 1). No *tmexCD1-toprJ1*-positive isolates were detected in pig fecal samples (Fig. 2(a) and Table S1). In addition, we retrieved the genomes of eight human *tmexCD1-toprJ1*-positive strains from our local database. In summary, a total of 153 isolates were identified, including *K. pneumoniae* (*n* = 144), *K. variicola* (*n* = 1), *K. quasipneumoniae* (*n* = 4), *K. michiganensis* (*n* = 2), or *K. oxytoca* (*n* = 2) (Table S4 in Appendix A).

There were 240 *tmexCD1-toprJ1*-containing genomic DNA sequences that were obtained from the GenBank database (accession numbers are provided in Table S5 in Appendix A). Among these strains, 230 were collected from China, and three strains were collected from Japan, three from Vietnam, two from Kenya, one from Republic of Korea, and one from Thailand (Fig. S1 in Appendix A). The *tmexCD1-toprJ1*-positive isolates were identified from various sources, including humans (*n* = 92), chicken feces (*n* = 84), swine feces and pig carcasses (*n* = 49), environmental samples (*n* = 9), duck feces (*n* = 3), flies (*n* = 2), pork (*n* = 1), and dogs (*n* = 1). A total of eight bacterial species were identified, including *K. pneumoniae* (*n* = 198), *E. coli* (*n* = 8), *K. quasipneumoniae* (*n* = 27), *K. similipneumoniae* (*n* = 2), *Raoultella ornithinolytica* (*R. ornithinolytica*, *n* = 2), *R. planticola* (*n* = 1), *Enterobacter hormaechei* (*E. hormaechei*, *n* = 1), and *Citrobacter youngae* (*C. youngae*, *n* = 1) (Table S4). All ten of the *tmexCD1-toprJ1*-positive strains collected from Japan, Republic of Korea, Vietnam, Kenya, and Thailand were identified as *K. pneumoniae* strains of human origin.

We also included 455 *tmexCD1-toprJ1*-positive Enterobacterales strains from our prior studies, comprising *K. pneumoniae* (*n* = 423), *K. oxytoca* (*n* = 22), *R. planticola* (*n* = 5), *K. variicola* (*n* = 2), *K. quasipneumoniae* (*n* = 1), *C. portucalensis* (*n* = 1), and *R. ornithinolytica* (*n* = 1) (Table S4). Thus, 848 *tmexCD1-toprJ1*-positive strains were analyzed in this study (Fig. S1), including 765 (90.2%) *K. pneumoniae*, 34 (4.0%) *K. quasipneumoniae*, 24 (2.8%) *K. oxytoca*, eight (0.9%) *E. coli*, six (0.7%) *R. planticola*, three (0.4%) *K. variicola*, three (0.4%) *R. ornithinolytica*, two (0.2%) *K. michiganensis*, one *C. youngae*, one *C. portucalensis*, and one *E. hormaechei* (Fig. 2(b) and Table S4). Among the 848 *tmexCD1-toprJ1*-positive strains, 102 isolates were collected from human samples, including blood (*n* = 24), urine (*n* = 16), sputum (*n* = 15), secretions (*n* = 5), tissue (*n* = 4), intestinal samples (*n* = 4), feces (*n* = 3), bronchoalveolar lavage fluid (*n* = 3), rectal swabs (*n* = 2), bile (*n* = 2), dialysate (*n* = 1), shunt fluid (*n* = 1), alveolar lavage (*n* = 1), and unknown samples (*n* = 21). Six bacterial species were identified among the human-derived isolates, including 93 *K. pneumoniae*, three *K. quasipneumoniae*, two *K. michiganensis*, two *K. oxytoca*, one *C. youngae*, and one *E. cloacae* (Tables S4–S6 in Appendix A). The majority of the *tmexCD1-toprJ1*-positive isolates were identified after 2016, with the earliest clinical isolates found in China in 2009. From 2009 to 2021, the number of human-derived *tmexCD1-toprJ1*-positive isolates showed an increasing trend, peaking in 2021 and then declining (Fig. 2(c)). The earliest isolates of chicken and swine originated from 2013 and 2019, respectively (Table S5). Combining the data from this study with our previous research, we found that from 2018 to 2022, the detection rate of chicken-derived *tmexCD1-toprJ1*-positive isolates decreased significantly, from 57.9% to 0 (Fig. 2(d)).

Given that both this study and prior research indicated a prevalence of *tmexCD1-toprJ1* in chicken farms, a scarcity of positive bacteria from pigs, and that *tmexCD1-toprJ1* is primarily carried by *K. pneumoniae*, we hypothesized that the low carriage of *tmexCD1-toprJ1*-positive bacteria in swine may be related to the low colonization of *K. pneumoniae* in the intestines of pigs. To investigate this, we compared the detection rates of *K. pneumoniae* in pig and chicken fecal samples collected from different farms in China. We found that the carriage rate of *K. pneumoniae* in swine feces (1.4%, 16/1 180) was significantly lower than that in chickens (15.1%, 257/1 702) (Tables S2 and S3).

3.2. Antimicrobial susceptibility profiles of tmexCD1-toprJ1 strains

The MICs against 13 antimicrobials were determined for 608 *tmexCD1-toprJ1*-positive strains (153 from this study and 455 from previous studies). The results revealed that all of the *tmexCD1-toprJ1*-carrying isolates were resistant to tetracyclines (tigecycline, doxycycline, and tetracycline) and exhibited MDR profiles, including 99.7% for sulfamethoxazole-trimethoprim, 98.0% for ciprofloxacin, 96.3% for florfenicol, 88.4% for gentamicin, 84.7% for amikacin, 81.5% for cefoxitin, 68.5% for cefotaxime, and 58.8% for ceftazidime (Fig. 3(a)). Notably, 285 (47.3%) and 13 (2.1%) strains were resistant to colistin and imipenem, respectively, with 185 (30.8%) strains exhibiting a high level of resistance to colistin (MIC ≥ 32 mg·L^{-1}) (Fig. 3(b)). All of the strains were tigecycline-resistant, with more than 81.7% of the isolates having an MIC greater than 8 μg·mL^{-1} (Fig. 3(c)).

3.3. Genomic characteristics of tmexCD1-toprJ1-positive strains

The genomes of 511 *tmexCD1-toprJ1*-positive strains (448 *K. pneumoniae* strains and 63 other Enterobacterales) were analyzed in this study, including 240 strains derived from GenBank and 271 strains (250 *K. pneumoniae*, seven *K. oxytoca*, five *R. planticola*, three *K. quasipneumoniae* subsp. *quasipneumoniae*, two *K. quasipneumoniae* subsp. *similipneumoniae*, two *K. michiganensis*, one *C. portucalensis*, and one *K. quasivariicola*) obtained in this and previous studies. Among the 448 *K. pneumoniae* strains, 93 were recovered from humans, 265 from chicken feces, 24 from swine, nine from pork, 11 from chicken meat, 19 from chicken farm environments, ten from duck feces, two from houseflies, and one each from geese, vegetables, and dogs (Table S4).

The 448 *tmexCD1-toprJ1*-positive *K. pneumoniae* isolates were categorized into 68 STs, with CC37 (including ST37 (*n* = 84) and its single locus variant ST726 (*n* = 48), ST896 (*n* = 20), and others (*n* = 12)) identified as the dominant clone, accounting for 36.6% (164/448). Other prevalent clones included ST15 (*n* = 41, 9.2%), ST11 (*n* = 33, 7.4%), ST1 (*n* = 26, 5.8%), and ST147 (*n* = 22, 4.9%). The ST37 *K. pneumoniae* strains were widely distributed and recovered from 11 sources across 15 provinces or cities in China. Among human-derived samples, the predominant ST types were ST15 (24.5%, *n* = 25), ST22 (11.8%, *n* = 12), ST37 (10.8%, *n* = 11), and ST11 (9.8%, *n* = 10). In chicken-derived *K. pneumoniae* strains, the most common STs were ST37 (20.6%) and ST726 (14.8%), followed

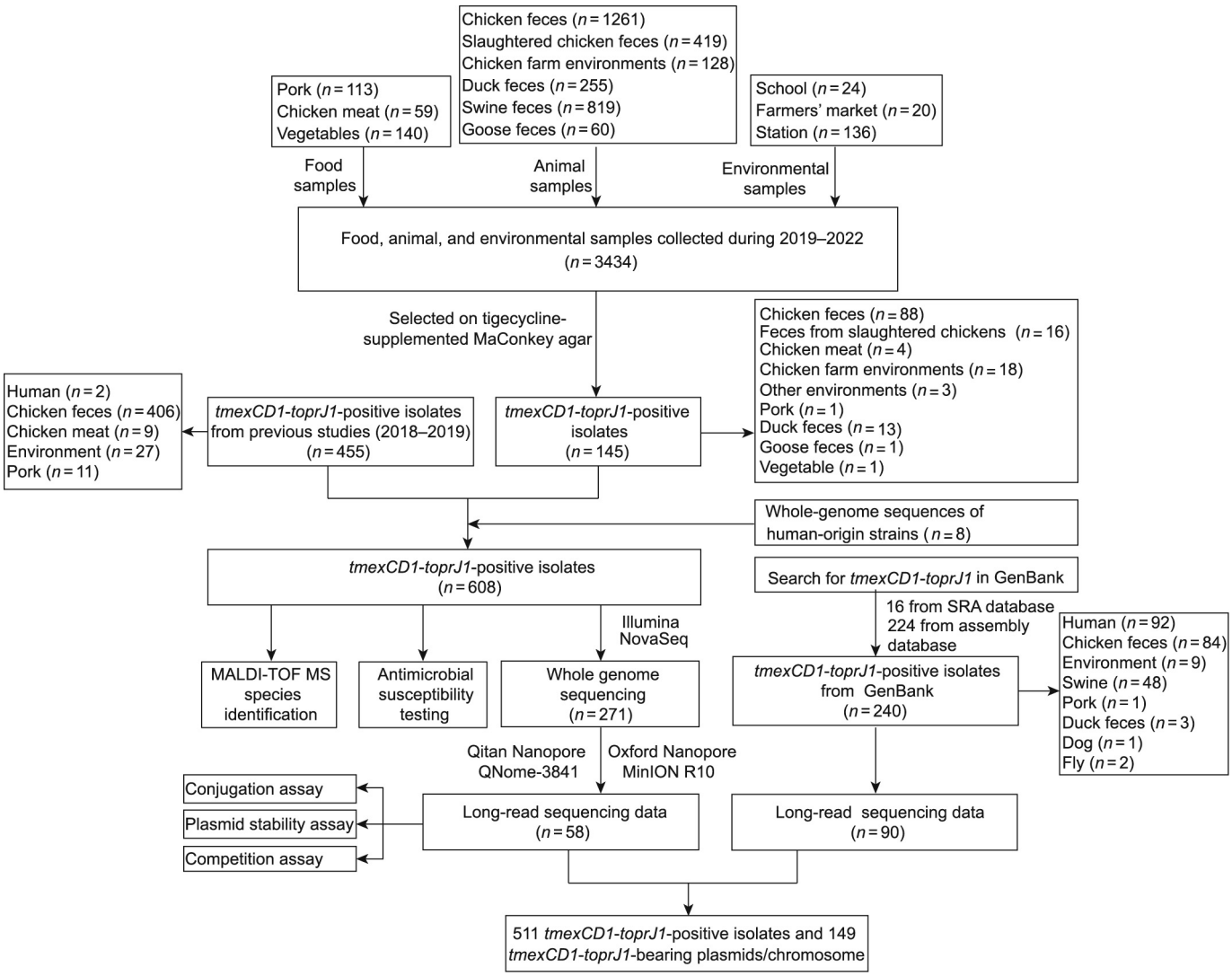

Fig. 1. Schematic diagram of the research workflow. The flowchart illustrates the selection and analysis process of *tmexCD1-toprJ1*-positive isolates in this study. SRA: Sequence Read Archive.

by ST1 (8.6%), ST11 (6.5%), ST42 (6.2%), ST147 (5.8%), ST15 (4.5%), and ST395 (3.4%). Among *K. pneumoniae* strains derived from swine and swine carcasses, the dominant ST types were ST896 (58.3%, 14/24) and ST11 (12.5%, 3/24), with other ST types accounting for 29.2% (7/24) (Fig. S2 in Appendix A). Outside China, among the ten *K. pneumoniae* strains, ST15 is the predominant strain (n = 4), followed by ST273 (n = 2), ST22, ST3332, ST2325, and ST709, each represented by a single isolate.

3.4. Resistome of tmexCD1-toprJ1-positive strains

All 511 of the *tmexCD1-toprJ1*-positive strains carried multiple ARGs, with a mean of 23.2 ARGs per isolate. The mean number of ARGs in the 448 *tmexCD1-toprJ1*-positive *K. pneumoniae* isolates was 26.4, which was significantly greater than that in clinical *K. pneumoniae* isolates producing *K. pneumoniae* carbapenemases (KPC) (average ARG number of 14.1) or New Delhi metallo-beta-lactamase (NDM) (19.7) (Fig. 3(d)). The dominant resistance genes among *tmexCD1-toprJ1*-positive strains included the aminoglycoside resistance gene *armA*, the florfenicol resistance gene *floR*, β-lactam resistance genes ($bla_{\text{DHA-1}}$ and $bla_{\text{CTX-M}}$), and the quinolone resistance gene *qnrB*, with prevalences of 78.5%, 79.5%, 82.2%, 59.1%, and 89.6%, respectively (Fig. 3(e) and Fig. S3 in Appendix A). Notably, 157 (109 from chicken feces, 28 from humans, 11 from chicken farm environments, and nine from other samples) colistin resistance genes (*mcr-8*, *mcr-1*, and *mcr-3*) were identified in *tmexCD1-toprJ1*-carrying strains, and *mcr-8* (n = 131) was the most common *mcr* gene. Further, 100 strains (36 from humans, 31 from chicken feces, 11 from chicken farm environments, 15 from swine feces, and seven from other samples) carried carbapenem resistance genes, including bla_{NDM} (17.2%, n = 88) (Fig. 3(e)), bla_{KPC} (4.1%, n = 21), bla_{IMP} (n = 2), $bla_{\text{OXA-181}}$ (n = 4), and co-occurring bla_{KPC} and bla_{NDM} (n = 15). Notably, 35 of the 100 *tmexCD1-toprJ1*-positive CREs also carried the *mcr* gene (*mcr-1*, *mcr-8*, or *mcr-3*). Among the 102 strains isolated from healthcare settings, 35.3% (n = 36) simultaneously carried carbapenem resistance genes and 27.5% (n = 28) harbored colistin resistance genes. In addition, in human-derived *K. pneumoniae*, the carriage rate of the *floR* gene in *tmexCD1-toprJ1*-positive strains (56.0%) was significantly greater than that in human-derived NDM (6.3%) and KPC-producing (4.2%) strains (Fig. 3(f)). The positive rates of heavy metal resistance genes, including the *sil*, *ter*, *pco*, *ars*, and *mer* clusters, among the *tmexCD1-toprJ1*-positive strains were 65.8%, 65.0%, 61.1%, 40.9%, and 39.3%, respectively (Fig. S4 in Appendix A), indi-

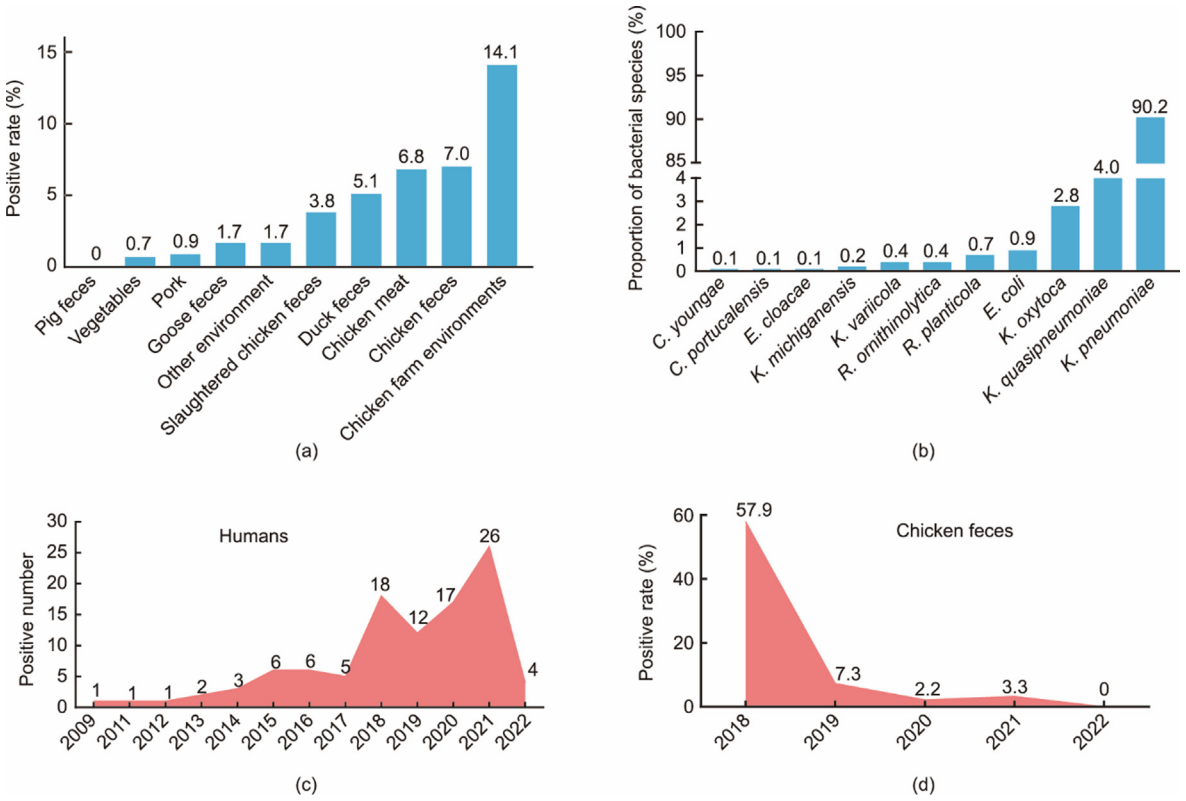

Fig. 2. Distribution of *tmexCD1-toprJ1*-positive Enterobacterales. (a) Positive rate of *tmexCD1-toprJ1*-positive strains isolated from nonhuman samples in this study. (b) Bacterial species of 848 *tmexCD1-toprJ1*-positive strains. (c) Changes in the number of human-derived *tmexCD1-toprJ1*-positive strains from 2009–2022. (d) Changes in the prevalence of *tmexCD1-toprJ1*-positive strains in chicken feces from 2018–2022.

cating that *tmexCD1-toprJ1*-positive strains frequently carry multiple ARGs and heavy metal resistance genes. Further, amino acid substitutions in GyrA, ParC, and MgrB, which mediate high levels of resistance to fluoroquinolones or colistin, were present in 350 (86.4%), 345 (85.2%), and 18 (4.4%) of the 448 *K. pneumoniae* strains, respectively (Fig. S5 in Appendix A).

3.5. Polysaccharide and virulence factors in tmexCD1-toprJ1-positive strains

Among the 448 *K. pneumoniae* strains, 71 known K loci (KL) encoding the core capsule biosynthesis machinery were identified, with KL186 (n = 36), KL81 (n = 31), KL3 (n = 22), and KL45 (n = 18) being the most common (Fig. S6 in Appendix A). Ten KL types (KL166, KL24, KL46, KL12, KL112, KL113, KL138, KL155, KL157, and KL39) were unique to human strains, whereas the remaining 24 types were detected in strains derived from animals, food, or the environment. A smaller number of distinct O loci (n = 11) were observed, with O1/O2v2 (n = 154), O3b (n = 61), O1/O2v1 (n = 56), and OL101 (n = 49) being the most common, consistent with previous reports (Fig. S7 in Appendix A).

The carriage rates of virulence factors, such as aerobactin (*iuc1*, *iuc3*, and *iuc5*), yersiniabactin (*ybt* and *ICEkp*), salmochelin, and the mucoid phenotype (*rmpADC* and *ramA2*), in the 448 *K. pneumoniae* strains were 7.8% (n = 35), 4.0% (n = 18), 0.9% (n = 4), and 0.7% (n = 3), respectively (Fig. S8 in Appendix A). Significant differences in the carriage of virulence genes were detected between human-derived *K. pneumoniae* and those from other sources. Three *iuc*, *iroN*, and *rmpA2*-carrying K64-ST11 hypervirulent CRKP strains were recovered from humans. The *ybt* genes were associated with four ICE*Kp* genes, with ICE*Kp3* (n = 7) and ICE*Kp5* (n = 7) being the most common. ICE*Kp3* (n = 5) was predominantly found in human-derived strains, whereas ICE*Kp5* (n = 6) predominated in animal- and food-derived strains (Fig. S8).

3.6. Transmission of tmexCD1-toprJ1-carrying K. pneumoniae clones

We constructed a core-genome phylogenetic tree in order to elucidate the phylogenetic relationships among the 448 *tmexCD1-toprJ1*-carrying *K. pneumoniae* strains from various sources. Hierarchical Bayesian analysis of the population structure (hierBAPS) revealed seven major clades within these strains (Fig. S9 in Appendix A). Extensive diversity was observed among *tmexCD1-toprJ1*-positive ST726, ST37, ST15, and ST22 *K. pneumoniae* strains derived from diverse sources. However, a high degree of relatedness was noted among strains from different geographical regions and sample origins across multiple lineages.

Further analysis of SNP differences between *tmexCD1-toprJ1*-carrying *K. pneumoniae* strains indicated common clonal spread among chickens and their environments, extending to transmission between chickens and humans (Table S7 in Appendix A). For example, the ST37 *K. pneumoniae* strain SCH140121R (human, Sichuan, China, 2020) exhibited only 12 and 14 core genome single nucleotide polymorphisms (cgSNPs) compared to the strains XJ222 (chicken, Xinjiang, China, 2019) and SCH090637 (human, Sichuan, China, 2019), respectively. Similarly, the ST37 strain C5921 (Sequence Read Archive (SRA): SRS9414716, Beijing, China, 2019) exhibited 14, 17, and 17 cgSNP differences from SH9I002 (chicken, Shanghai, China, 2019), GD9I034T, and GD9I037T (chicken, Guangdong, China, 2019), respectively (Fig. S10 and Table S7 in Appendix A). The ST37 strain 13L165 (GCA_033433955, human, Sichuan, China, 2013) showed only 20 and 23 cgSNP differences from GHZ9P037 (pork, Guangdong, China, 2019) and GXQ9C223 (chicken, Guangxi, China, 2019), respectively.

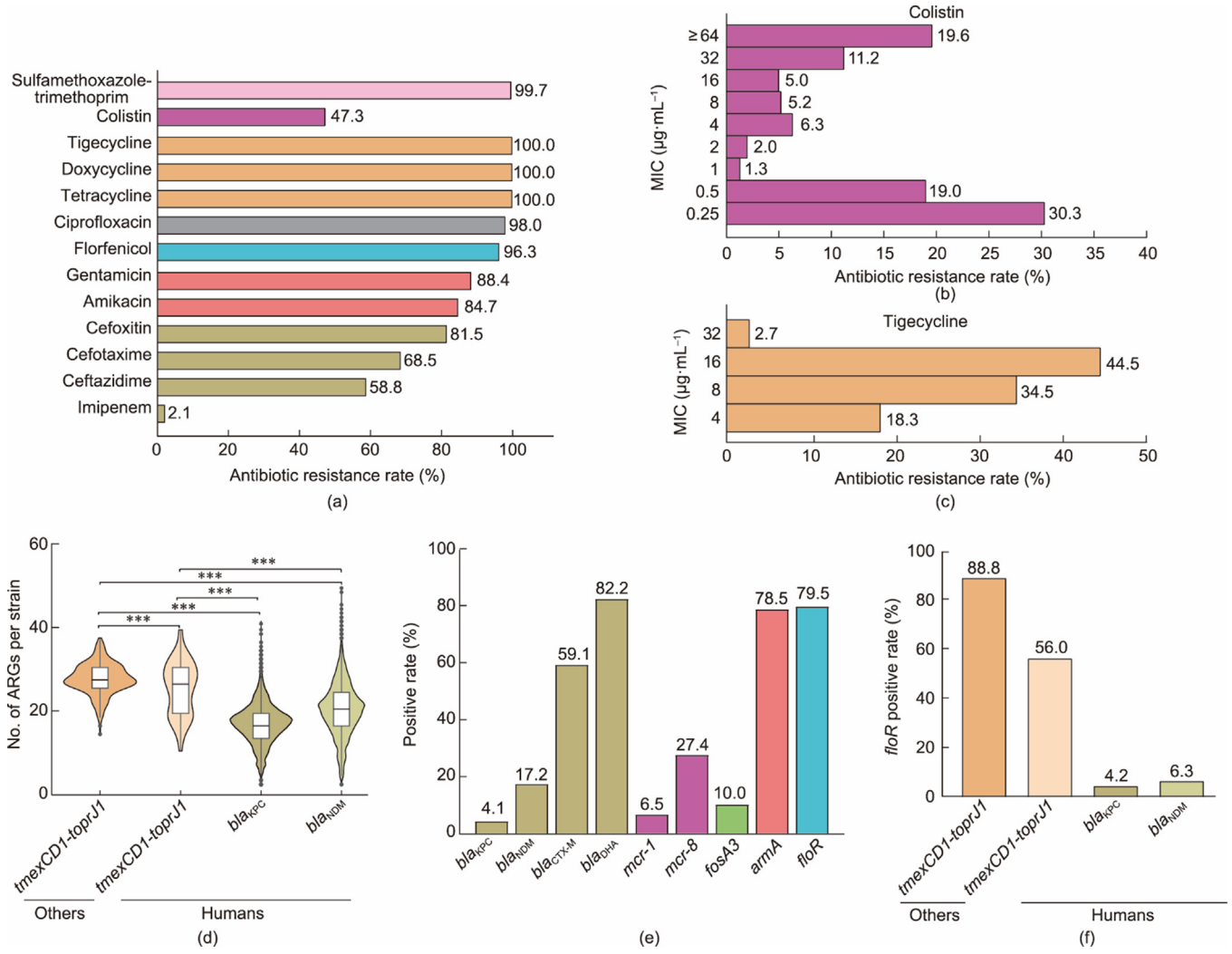

Fig. 3. Resistance phenotypes and genotypes of *tmexCD1-toprJ1*-positive strains. (a) Histogram of the resistance rates of the *tmexCD1-toprJ1*-positive strains in this study (n = 153) and previous studies (n = 455) to antimicrobial agents. Distribution of MIC values of (b) *tmexCD1-toprJ1* colistin and (c) tigecycline for *tmexCD1-toprJ1*-positive strains. (d) The average number of ARGs carried by *tmexCD1-toprJ1*, bla_{NDM}-, and bla_{KPC}-positive *K. pneumoniae* strains. The green and red violin plots represent *tmexCD1-toprJ1*-positive strains from humans (n = 93) and other sources (animals, foods, and environments, n = 335), respectively, whereas the purple and blue violin plots represent bla_{KPC} (n = 5 597) and bla_{NDM} (n = 15 534)-positive strains, respectively. *** indicates statistically significant differences between two groups ($p < 0.001$); No.: numbers. (e) Positive rate of ARGs in 511 *tmexCD1-toprJ1*-positive strains. (f) Prevalence of the *floR* gene in *tmexCD1-toprJ1*, bla_{NDM}, and bla_{KPC} positive *K. pneumoniae*. The two red columns represent *tmexCD1-toprJ1* positive strains from humans (n = 93) and other sources (animals, foods, and environments, n = 335), whereas the yellow and blue bars represent bla_{KPC}-positive (n = 5 597) and bla_{NDM}-positive (n = 15 534) *K. pneumoniae* strains obtained from humans, respectively.

Further, closely related strains of ST42, ST147, and ST1 were found among *tmexCD1-toprJ1*-carrying *K. pneumoniae* clones isolated from chickens and their environments. Six ST4523–KL111 strains with 0–13 cgSNP differences were isolated from chicken feces, slaughtered chickens, or retail chicken meat in Fujian and Guangdong Provinces. This suggests the vertical transmission of *tmexCD1-toprJ1* through poultry processing and the food chain (Fig. S10 and Table S7).

Notably, the ST22 *tmexCD1-toprJ1*-positive strain SH9C008 (retail chicken, Shanghai, China, 2019) exhibited only 15–32 cgSNP differences compared to ten strains isolated from a hospital in Beijing between 2018 and 2021. Similarly, the ST15 strain AHM8C074 collected from chicken feces in 2018 showed minimal SNP differences (ranging from 17 to 40) with various human-derived strains from different regions and years. The globally prevalent high-risk ST15 clone has been significantly implicated in the dissemination of *tmexCD1-toprJ1*. Our analysis revealed that the *tmexCD1-toprJ1*-positive ST15 strain SRY643 (GenBank No. GCA_033861315, 2021) from a patient in Zhejiang, China, exhibited only eight base pair variations in cgSNPs compared to a human-derived ST15 strain from Japan, JBEAACG-19-0050 (DRR390524, 2019). Further, two ST15 strains (GCA_024990835 and GCA_014117765) collected from Kenya in 2017 were closely related to two human-derived strains (GCA_034737695 and GCA_034737815) from Guangxi, China, with only 19–24 cgSNP differences, indicating the clonal spread of *tmexCD1-toprJ1*-positive ST15 across countries (Fig. S10 and Table S7).

ST37 *K. pneumoniae*, which accounted for the highest percentage of all of the *tmexCD1-toprJ1*-positive strains, was selected as a representative for analyzing the genetic relationships of *tmexCD1-toprJ1*-positive and -negative strains from different origins. We obtained the genomic sequences of 1 412 ST37 *K. pneumoniae* strains, 81 of which were *tmexCD1-toprJ1*-positive. Core-genome phylogenetic analysis revealed 11 clades among the 1 412 ST37 strains. Among the 81 *tmexCD1-toprJ1*-positive ST37 strains, all except one (KP294, CP083445, isolated from a human in Chongqing, China) were distributed across two clades, primarily comprising strains collected from animals or environmental sam-

ples (Fig. S9 in Appendix A). Notably, ten out of the 11 *tmexCD1-toprJ1*-positive ST37 strains originating from healthcare settings were found in these two clades, suggesting that these healthcare-associated strains may have been derived from animals.

3.7. Epidemiological characteristics of tmexCD1-toprJ1-harboring plasmids

We obtained the complete sequences of 148 *tmexCD1-toprJ1*-bearing plasmids (58 from this study and 90 from GenBank) and one *tmexCD1-toprJ1*-bearing chromosome (Tables S8 and S9 in Appendix A). A total of 24 plasmid types were identified among the 148 *tmexCD1-toprJ1*-bearing plasmids, with IncFIB(Mar)–IncHI1B (33.8%, n = 50) being the predominant vector, followed by IncFIB(K)–IncHI1B (22.3%, n = 33), IncFIA–IncFII(K) (8.1%, n = 12), IncU–IncHI5 (5.4%, n = 8), and IncFIB(K)–IncFII(K) (4.7%, n = 7) (Fig. 4(a); Tables S8 and S9).

The IncFIB(Mar)–IncHI1B plasmid, commonly found in *K. pneumoniae* (Fig. 4(b)), is a conjugative and MDR plasmid. *tmexCD1-toprJ1*-carrying IncFIB(Mar)–IncHI1B plasmids, sharing a highly conserved backbone and an MDR region with coverage and similarity > 98%, were detected in various *Klebsiella* species. Distinct ST profiles of *K. pneumoniae* from chickens, swine, meat, the environment, houseflies, and humans in China and Vietnam were identified (Fig. 4(a); Tables S8 and S9). The pMH15-269M_1 plasmid (AP023338.1) collected from a human in Vietnam was highly similar (99% coverage and 99.84% identity) to the pHN111RT-1 plasmid (MT647838.1) isolated from sewage in China, indicating the spread of *tmexCD1-toprJ1*-carrying IncFIB (Mar)–IncHI1B plasmids between China and Vietnam. *tmexCD1-toprJ1* was commonly associated with $bla_{\text{DHA-1}}$ (94.0%, 47/50), *armA* (82.0%, 41/50), *qnr* (92.0%, 46/50), and *mcr-1* (8.0%, 4/50) located in an MDR region flanked by incomplete Tn*1721* in IncFIB(Mar)–IncHI1B plasmids (Fig. S11 in Appendix A).

The *tmexCD1-toprJ1*-bearing IncFIB(K)–IncHI1B plasmid, also prevalent in *K. pneumoniae* (Fig. 4(b)), shares a less conserved backbone and a relatively conserved MDR region containing $bla_{\text{DHA-1}}$, *armA*, *qnrB*, and *aac(3)-IV*, etc. (Fig. S12, Tables S8 and S9 in Appendix A), which is highly similar to the MDR region in the IncFIB (Mar)–IncHI1B plasmid. However, all of the IncFIB(K)–IncHI1B-type plasmids were non-conjugatable due to the absence of type IV secretion systems (T4SSs). Like the IncFIB(Mar)–IncHI1B plasmids, *tmexCD1-toprJ1*-carrying IncFIB(K)–IncHI1B plasmids were detected in *K. pneumoniae* or *K. quasivariicola* from various geographical locations and sources (human, chicken feces, duck feces, and environment). Most IncFIB(K)–IncHI1B plasmids were identified in CG37 (42.4%; ST37, n = 10; ST726, n = 4) and CG15 (24.2%; ST15, n = 8) (Fig. 4(a)), suggesting host specificity for *tmexCD1-toprJ1*-bearing plasmids.

In addition, *tmexCD1-toprJ1*-carrying IncFIA–IncFII(K) (n = 12), IncFIB(K)–IncFII(K) (n = 7), and IncFII(K) (n = 5) plasmids were conjugatable but carried fewer ARGs (Fig. S13, Table S8 and S9 in Appendix A). These plasmids also harbored *mcr-8* and shared a relatively conserved backbone sequences with pHNAH8I-1 (MK347425), which exhibited > 98% similarity (Fig. S13). They were mainly obtained from chicken feces or chicken farm environments, except the IncFIA–IncFII(K)-type plasmid pKQBSI104-1 and the IncFIB(K)–IncFII(K)-type plasmid pKP15ZE495-1 collected from humans.

Eight IncU–IncHI5 plasmids were distributed among six bacterial species: *K. pneumoniae* (n = 1), *K. michiganensis* (n = 2), *K. oxytoca* (n = 1), *K. quasipneumoniae* (n = 1), *R. planticola* (n = 2), and *E. cloacae* (n = 1) (Fig. 4(a)). This suggests that IncU–IncHI5 plasmids play a significant role in the cross-species transmission of the *tmexCD1-toprJ1* gene cluster. The IncU–IncHI5 plasmids also carried other ARGs, including $bla_{\text{NDM-1}}$ (n = 2), $bla_{\text{IMP-4}}$ (n = 2), *armA*, and *qnrS1* (Fig. S14 in Appendix A). Sequence comparisons revealed that seven *tmexCD1-toprJ1*-carrying IncU–IncHI5 plasmids had similar plasmid backbone structures and variable regions, except that pHNSCH140054-1 and pHNSCH140055-1 lacked a transfer region (Fig. S14).

In addition to these plasmids, we identified five MDR hybrid plasmids, including IncFIA–IncFIB(K)–IncHI1B–IncR (n = 1) and IncFIA–IncFIB(K)–IncHI1B (n = 4), which were the first to carry *tmexCD1-toprJ1* (Fig. 4(a)). The four IncFIA–IncFIB(K)–IncHI1B plasmids were associated with ST37 (n = 3) or ST15 (n = 1) *K. pneumoniae* strains. Comparisons of these five hybrid plasmids with IncFIB (K)–IncHI1B plasmids revealed similar backbones and variable regions.

We further assessed the transferability and stability of the dominant *tmexCD1-toprJ1*-carrying plasmids: IncFIB(K)–IncHI1B, IncFIB(Mar)–IncHI1B, IncU–IncHI5, and IncFII(K)–IncFIA, in *E. coli* and *K. pneumoniae*. Conjugation assays demonstrated that these plasmids could be transferred to *E. coli* J53 at frequencies ranging from approximately 5.24×10^{-6} to 3.05×10^{-4} (Fig. S15 in Appendix A), except for the IncFIB(K)–IncHI1B plasmid, which was non-conjugative. Stability assays revealed that in wild-type strains (Fig. 4(c)), the IncFIA–IncFII(K) and IncFII(K) plasmids were maintained for 15 d. However, the IncFIB(K)–IncFII(K), IncU–IncHI5, IncFIB(Mar)–IncHI1B, and IncFIB(K)–IncHI1B plasmids exhibited significant loss beginning on day 3 or 6, with loss rates exceeding 50% by day 15. In *K. pneumoniae* AH58I (Fig. 4(d)), the IncFIA–IncFII(K) plasmids were stably maintained, with an IncFII(K) plasmid loss rate of 30%, whereas the loss rates for the IncFIB (Mar)–IncHI1B and IncU–IncHI5 plasmids ranged from 50% to 90%. In *E. coli* J53 (Fig. 4(e)), the loss rates of the IncFII(K) and IncFIB (K)–IncFII(K) plasmids were 30%, whereas those of the IncFIB (Mar)–IncHI1B, IncU–IncHI5, and IncFIB(K)–IncFII(K) plasmids exceeded 50%. Overall, *tmexCD1-toprJ1*-carrying plasmids exhibited significant fitness costs to both *K. pneumoniae* AH58I and *E. coli* J53, with a lower fitness cost observed in *K. pneumoniae* AH58I compared to *E. coli* J53. The RF of IncFIB(Mar)–IncHI1B, IncFIB(K)–IncFII(K), IncFIA–IncFII(K), IncU–IncHI5, and IncFII(K) in *E. coli* J53 decreased from 0.9 to 0.2 over 24–96 h, whereas in *K. pneumoniae* AH58I, the RF decreased to approximately 0.4–0.7 (Figs. 4(f) and (g)).

3.8. Genetic context features of tmexCD1-toprJ1

To characterize the genetic contexts surrounding *tmexCD1-toprJ1*, we conducted a comparative analysis of plasmids from this study and GenBank, revealing ten distinct types of genetic environments (Fig. S16 in Appendix A). Among these, types I-1, II-1, and III represent common structures, while three novel genetic contexts were identified.

3.8.1. Type I structures

The type I translocatable unit features the core structure *int1-int2-hp1-hp2-tnfxB1-tmexCD1-toprJ1*, marking it as the earliest reported genetic structure of *tmexCD1-toprJ1*. This unit is classified as a strand-biased circularizing integrative element (SE) [45] and is designated as SE-pHNAH8I. We identified the complete SE-pHNAH8I gene in 37 plasmids: 19 from this study and 18 from GenBank, spanning ten plasmid types, including IncFIA–IncFII(K) (n = 11) and IncFIB(K)–IncFII(K) (n = 6), IncFII(K) (n = 5), IncU–IncHI5 (n = 8), and others (n = 7) (Fig. 4(a)). Notably, SE-pHNAH8I was integrated into the *tnpA* gene of Tn*5393*/Tn*5393C*, with a consistent potential integration site (ATCT), indicating its mobility. Within the IncU–IncHI5 plasmids, Tn*5393* was inserted between transposons Tn*1721* and Tn*5563*. Variations from types I-1 to I-5 differ depending on whether Tn*5393* is truncated or disrupted by additional insertion sequences.

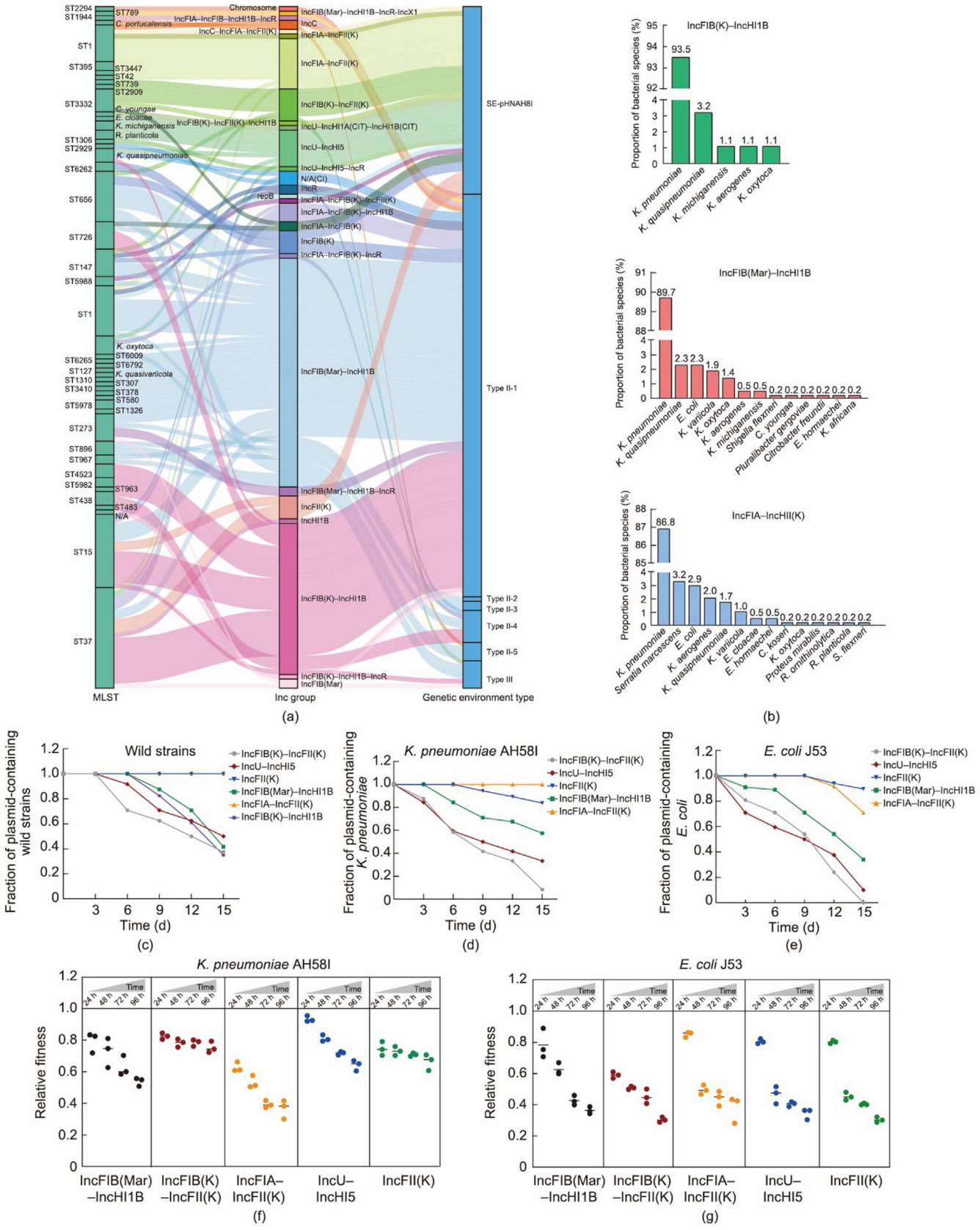

Fig. 4. Characteristics of *tmexCD1-toprJ1*-carrying plasmids. (a) Sankey diagram combining the bacterial species (*K. pneumoniae* shown by ST type), plasmid replicon types, and genetic environments of *tmexCD1-toprJ1* on the basis of information from the 149 sequenced plasmids (86 were retrieved from the NCBI database, and 63 were sequenced in this study). The diameter of the line is proportional to the number of strains. Lines are colored according to the plasmid replicon type. (b) Host bacterial species distributions of the IncFIB(K)–IncHI1B, IncFIB(Mar)–IncHI1B, and IncFIA–IncFII(K) plasmids in the NCBI NT database (identity ≥ 97% and query coverage ≥ 70%). Stability of different *tmexCD1-toprJ1*-carrying plasmids in (c) wild-type *K. pneumoniae* strains, (d) *K. pneumoniae* AH58I strains, and (e) *E. coli* J53 strains. RF of *tmexCD1-toprJ1*-carrying IncFIB(Mar)–IncHI1B, IncFIB(K)–IncFII(K), IncFIA–IncFII(K), IncU–IncHI5, and IncFII(K) plasmids in (f) *K. pneumoniae* AH58I, and (g) *E. coli* J53.

3.8.2. Type II structures

Type II structures serve as the primary genetic environments for *tmexCD1-toprJ1* and are predominantly found on MDR plasmids (Fig. 5(a)). We identified these structures in 103 plasmids, categorizing them into five substructures, with type II-1 being the most prevalent. The key difference between type II-1 and types II-2 to II-5 is the presence of insertion sequences such as IS*CR1*, IS*1294*, or IS*26*, which truncate the upstream or downstream segments of type II-1. The type II-1 structure, organized as IS*26*-*Δhp2-tnfxB1-tmexC1-tmexD1-toprJ1-strAB*-ΔIS*903B*-*Δmcp*-IS*26*, was observed in 86 plasmids, one *K. pneumoniae* chromosome, and two IS*26*-mediated circular intermediates. The predominant plasmid types carrying this structure included IncFIB(Mar)–IncHI1B (n = 39) and IncFIB(K)–IncHI1B (n = 29), followed by IncFIB(K)–IncHI1B–IncFIA (n = 4), IncFIB(K) (n = 3), IncR (n = 2), IncFIB(Mar)–IncHI1B–IncR (n = 2), and others (n = 6) (Fig. 4(a) and Fig. 5(a)).

3.8.3. Type III structures

The type III structure, represented as IS*26*-*Δhp1-tmexCD1-toprJ1*-ΔTn*5393* (*ΔtnpA-tnpR-strB-strA*)-Tn*501*, was primarily identified in strains of swine origin and was found in only six plasmids from various Inc groups (Fig. 4(a) and Fig. 5(a)).

3.8.4. Trends and observations

In total, we identified 99 type I structures, 255 type II structures, seven type III structures, and two other types from *tmexCD1-toprJ1*-carrying contigs extracted from assembled sequences. The proportion of type II structures rose significantly from 0.27% in 2018 to 87% in 2022, demonstrating a steady increase, particularly in human-derived strains, compared to those from animals and the environment. Among the nine *tmexCD1-toprJ1*-positive strains isolated between 2008 and 2014, seven exhibited type I structures, two had type III structures, and none contained type II structures (Fig. 5(b)).

3.8.5. Formation of type II genetic environments

To investigate the formation of type II genetic environments (Fig. 5(c)), we blasted sequences of the fragment ΔTn*1721*-ΔIS*903-strA-strB-tnpR* found in type II-1. This search revealed an identical sequence in the IncR plasmid pWP3-W18-ESBL-01_2 (GenBank accession number: AP021971, *R. ornithinolytica*, Japan: Tokyo, 2018). In this plasmid, two transposons, Tn*1721* and Tn*5393*, were inserted into IS*903*, forming direct repeats (DRs) ATTAA and GCTAT (Fig. 5(c), structure II). A similar structure was also present in the IncR-type plasmid pYTF44-1-tmexCD (GenBank No. CP075287), which carries *tmexCD1-toprJ1*, but with additional resistance genes and insertion sequences within Tn*1721*. We hypothesized that the type II-1 structure originated from SE-pHNAH8I capturing the *tmexCD1-toprJ1* gene cluster, subsequently integrating into the *tnpA* gene of Tn*5393* in an IncR plasmid similar to pWP3-W18-ESBL-012. The *hp1* gene in SE-pHNAH8I was truncated by IS*26*, and the *mcp* gene of Tn*1721* was also inserted by IS*26*, leading to the formation of a new structure. Following multiple insertion, deletion, and recombination events mediated by diverse insertion sequences, the structure of the pYTF44-1-*tmexCD* plasmid emerged, generating a type II-1-like structure. The presence of IS*26* at both ends of the type II-1 structure facilitated the formation of cyclic intermediates, allowing for the transfer between plasmids within the same cell. This suggests that the type II-1 genetic structure was initially generated in an IncR plasmid and later transferred to IncFIB(MAR)–IncHI1B and IncFIB(K)–IncHI1B plasmids. The type II-2 and type II-3 structures were newly identified and resembled the type II-1 structure driven by IS*26* or IS*CR1*.

3.8.6. Ancestral structure of type III

Further BLAST analysis revealed the structure of Tn*501*–Tn*5393* on plasmid pAAA83 (AB852526), leading us to speculate that this may represent the ancestral structure of type III. We propose a model for the formation of type III: initially, SE-pHNAH8I is integrated into Tn*5393*, followed by the insertion and rearrangement of IS*26* and IS*4321*, resulting in the type III structure. The emergence of various *tmexCD1-toprJ1*-harboring genetic elements illustrates the diverse mechanisms of *tmexCD1-toprJ1* transfer among different plasmids.

4. Discussion

Tigecycline is a vital antibiotic for treating infections caused by MDR bacteria. The emergence of the tigecycline resistance gene cluster *tmexCD1-toprJ1* presents significant therapeutic challenges in clinical settings. This study offers the first comprehensive analysis of the epidemiological distribution and evolutionary transmission vectors of *tmexCD1-toprJ1* in China and globally, which will aid in the development of relevant interventions.

Previous research has indicated that *tmexCD1-toprJ1*-positive strains are predominantly found in *K. pneumoniae* and related genera from chicken farms in China [16,46]. Our findings corroborate these reports, revealing that *tmexCD1-toprJ1* is mainly distributed among *K. pneumoniae* strains on domestic chicken farms [16,29,46]. However, its presence has expanded beyond China, with detections reported in Japan [47], Republic of Korea, Thailand, Vietnam [48], and Kenya, across various ecological niches, including chicken, duck, food, pigs, river water, sewage, vegetables, fish, and humans [16,28–30,46,48–50], and in diverse Enterobacterales, including *E. coli*, *C. portucalensis*, *C. youngae*, and *E. cloacae* [18,46,48–52]. Given that *tmexCD1-toprJ1* was first discovered in animals and that it is detected more frequently in animals than in humans, we propose that its origin likely lies in animals, with subsequent transmission to humans [18,28,50–52]. Notably, although *tmexCD1-toprJ1*-positive strains are rarely found in swine, the significantly lower carriage rate of *K. pneumoniae* in pig intestines (1.4%) compared to chickens (15.1%) may reflect specific epidemiological characteristics of the *tmexCD1-toprJ1* gene cluster, warranting further investigation.

Our study also highlighted that *tmexCD1-toprJ1*-positive strains exhibit a high resistance rate to most antimicrobial agents and carry significantly more resistance genes than bla_{NDM}- and bla_{KPC}-positive bacteria. All of the *tmexCD1-toprJ1*-positive strains exhibited an MDR phenotype, particularly demonstrating high resistance to colistin, despite a notable decline in colistin resistance among *E. coli* in animals and humans following the colistin withdrawal policy in China in 2017 [53,54]. Interestingly, the *tmexCD1-toprJ1*-carrying strains collected after 2017 still exhibited substantial colistin resistance. The frequent occurrence of *mcr-8* in these strains could be attributed to the fact that *Klebsiella* spp. is their primary host [55,56]. *K. pneumoniae* is the most notorious pathogen in both hospital and community settings, contributing to one-third of all of the healthcare-associated gram-negative infections worldwide [57,58]. Alarmingly, the acquisition of AMR determinants, particularly those conferring resistance to third-generation cephalosporins and carbapenems, in *K. pneumoniae* has increased in recent decades [59], leaving colistin and tigecycline as the few effective drugs. Thus, the co-existence of the *tmexCD1-toprJ1* and *mcr* genes in *K. pneumoniae* poses challenges in healthcare settings, requiring ongoing vigilance.

In addition to the *mcr* gene, *tmexCD1-toprJ1*-positive strains also harbor carbapenem resistance genes such as bla_{NDM} and bla_{KPC}, with some strains carrying multiple carbapenem resistance genes simultaneously [60,61]. Further, most *tmexCD1-toprJ1*-positive strains exhibited a higher prevalence of the florfenicol resistance gene *floR* compared to NDM- and KPC-producing *K. pneumoniae*, supporting the idea that these strains may have originated from

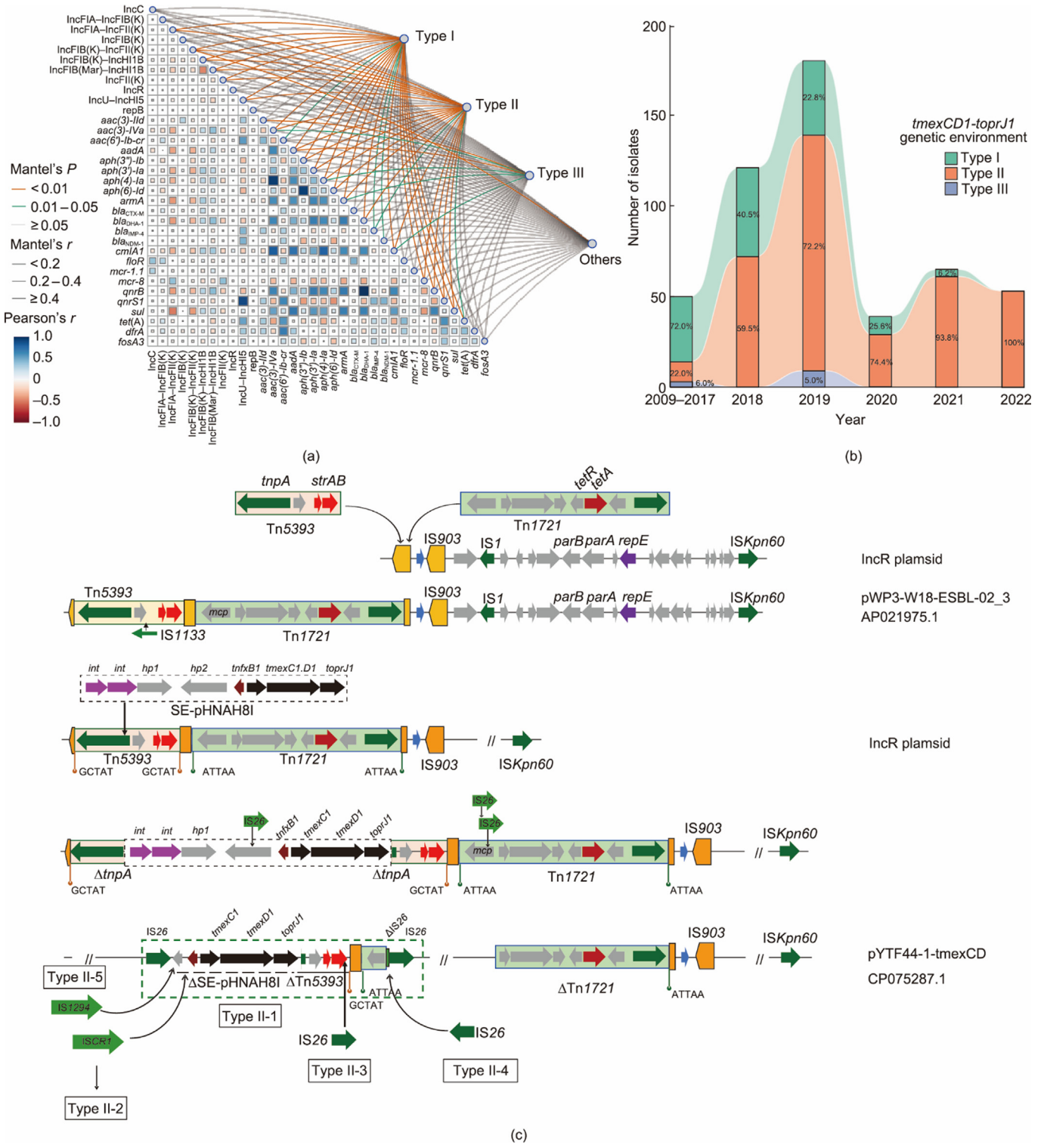

Fig. 5. Genetic structure of *tmexCD1-toprJ1*. (a) Correlation analysis of the genetic environments of *tmexCD1-toprJ1*, plasmids, and ARGs. The negative correlation and positive correlation are shown in red and blue squares, respectively. The thickness of the lines represents the strength of the correlation, with thicker lines indicating stronger correlations. For Mantel's *p* value, $p < 0.01$ is represented by orange lines, indicating a highly significant correlation; $p = 0.01–0.05$ is represented by green lines, indicating a significant correlation; and $p > 0.05$ is represented by gray lines, indicating a non-significant correlation. (b) Dynamics of changes in the genetic context of *tmexCD1-toprJ1* in 511 sequenced *tmexCD1-toprJ1*-positive strains from 2009 to 2022. (c) Formation model of the type II genetic environment of *tmexCD1-toprJ1*.

animals. Several strains also contain multiple heavy metal resistance genes, enhancing their persistence in environments with high antimicrobial and heavy metal pressures [62], typical of food animal production.

Despite the diversity observed in the phylogenetic tree, a close genetic relationship was noted among *tmexCD1-toprJ1*-positive *K. pneumoniae* strains from different ecological niches. Clonal transmission of the *tmexCD1-toprJ1* gene cluster was evident between chicken farms and retail chicken meat, suggesting potential transmission from chickens to humans via the food chain. The international high-risk ST15 *K. pneumoniae* clone is also implicated in the global spread of the *tmexCD1-toprJ1* gene cluster. In addition,

although previous studies reported limited clonal transmission of resistant strains between animals and humans [63], our findings revealed instances of clonal transmission of *tmexCD1-toprJ1*-positive ST37 *K. pneumoniae* across various years and ecological niches, including humans, chickens, and retail chicken meat. Notably, chicken-derived ST37 *K. pneumoniae* strains were closely related to human- and environment-derived strains carrying bla_{NDM} [64,65]. This differs from KPC-producing ST11 *K. pneumoniae* and CTX-M-producing ST131 *E. coli*, which are almost exclusively detected in strains originating from healthcare settings [66]. More importantly, we identified *tmexCD1-toprJ1* in KL64-ST11 highly virulent carbapenem-resistant *K. pneumoniae* (hv-CRKP), a strain prevalent in nosocomial outbreaks in China and Southeast Asia [67,68]. The concurrent presence of *tmexCD1-toprJ1* in hypervirulent, transmissible, and extensively drug-resistant KL64-ST11 hv-CRKP poses a severe threat to public health.

The narrow host range of *tmexCD1-toprJ1*-encoded plasmids may limit the dissemination of *tmexCD1-toprJ1* across different bacterial species. Our data indicate that the predominant vectors for *tmexCD1-toprJ1* are IncFIIk, IncFIBK–IncHI1B, and IncFIB (MAR)–IncHI1B, which are primarily found in *K. pneumoniae*. These types are characterized as narrow host range plasmids, making it less likely for *tmexCD1-toprJ1* to spread to other Enterobacterales (Fig. 4(b)). Given that *tmexCD1-toprJ1* emerged relatively recently (around 2009), it has likely not been widely transferred among plasmids. However, the association of *tmexCD1-toprJ1* with IS*26* [69], a common mobile element capable of carrying multiple drug resistance genes, has facilitated its spread to broad-host-range plasmids such as IncR, IncC, and IncU–IncHI5, potentially increasing the gene's dissemination [28,50,51]. Further, the identification of *tmexCD1-toprJ1* in *E. coli*, *E. cloacae*, and *Citrobacter* spp. demonstrated that *tmexCD1-toprJ1* has spread to other species [50,51], suggesting that across-species transmission is occurring, and that it has the potential for further dissemination.

Our findings confirm the significant role of SE [45], specifically SE-pHNAH8I, in the transmission of *tmexCD1-toprJ1*. While direct evidence of SE-pHNAH8I mobility is lacking, the presence of similar SE-pHNAH8I in various plasmid types suggests that multiple translocation events may have occurred. It is hypothesized that SE-pHNAH8I could mobilize *tmexCD1-toprJ1* into plasmids such as IncFIA–IncFII(K), IncFIBK–IncFII, and IncU–IncHI5. In addition, Tn*1721* and SE-pHNAH8I, located in the Tn*1721*-ΔIS*903*-Tn*5393*Δ-SE-pHNAH8I structure on the IncR plasmid, were truncated by two IS*26* elements, forming the type II-1 structure. These IS*26*-flanked pseudocomposite transposons are pivotal in disseminating resistance determinants in Gram-negative bacteria [69]. This may enable the *tmexCD1-toprJ1* gene cluster to jump into MDR IncFIB(K)–IncHI1B and IncFIB(MAR)–IncHI1B plasmids from IncR-type plasmids such as pYTF44-1-tmexCD. Despite the fitness costs associated with *tmexCD1-toprJ1*, its complex genetic environment may facilitate horizontal gene transfer across diverse plasmids and bacteria. Over time, the gradual transfer of *tmexCD1-toprJ1* into plasmids with additional resistance genes has enhanced its persistence, shifting from the less efficient SE-pHNAH8I to more mobile elements like IS*26*, which support the formation of circular intermediates [70].

Interestingly, the prevalence of *tmexCD1-toprJ1* in poultry has decreased significantly from 57.9% in 2018 to 0.7% by 2022. Zhao et al. [71] reported a decrease in tetracycline usage between 2018 and 2020, particularly following the ban on antimicrobial agents in animal feed as growth promoters, effective July 1, 2020 [71]. Thus, the decline of *tmexCD1-toprJ1* correlates with a substantial reduction in antibiotic use in food animals in China. This mirrors the reduction of the *mcr-1* gene prevalence among Enterobacterales in food animals after the colistin ban in China, which also led to lower *mcr-1* detection rates in human-derived strains [53,54,71]. Similarly, the decrease in *tmexCD1-toprJ1* detection among chickens corresponds with a notable reduction in human-derived *tmexCD1-toprJ1*-positive strains recorded in the GenBank database for 2022 and 2023, suggesting a direct relationship between animal and human prevalence. These findings underscore the critical role of reducing antibiotic usage in controlling the spread of resistance genes and highlight China's substantial efforts to combat AMR in animal reservoirs [53,54,71]. In addition, similar to *mcr-1* [72], the fitness cost associated with the *tmexCD1-toprJ1* gene may result in its loss when antibiotic selection pressure is absent, contributing to the observed decrease in detection rates. These findings underscore the critical role of reducing antibiotic usage in controlling the spread of resistance genes and highlight China's substantial efforts and achievements in combating AMR in animal reservoirs. Currently, *tmexCD1-toprJ1* is predominantly found in China, but its presence is increasing in neighboring Asian countries. The similarity between *tmexCD1-toprJ1*-positive strains and plasmids from these countries and those from China suggests potential cross-border spread, reinforcing the need for a One Health approach to address the global challenge of AMR.

Although our study provides evidence of cross-ecological transmission of *tmexCD1-toprJ1 K. pneumoniae* among chickens, food, and humans, we acknowledge several limitations in our research. First, the African swine fever outbreak in China, which has been ongoing since 2018, has hindered the collection of diverse pig fecal samples from various regions. Second, the coronavirus disease 2019 (COVID-19) pandemic severely restricted the collection of environmental samples. As a result, the number of pig and environmental samples in our study was relatively small, potentially introducing bias into the epidemiological data. We incorporated data from public databases, enabling us to demonstrate the prevalence trends of *tmexCD1-toprJ*1 and to provide more robust evidence of its transmission among animals, humans, and food sources.

5. Conclusions

In summary, this study represents the first comprehensive epidemiological surveillance of *tmexCD1-toprJ1*-positive Enterobacterales from a One Health perspective. Our findings indicate that *tmexCD1-toprJ1* is primarily endemic to chicken-derived *K. pneumoniae* on chicken farms and is rarely found in porcine strains, likely due to the narrow host range of *tmexCD1-toprJ1* plasmids and limited colonization of *K. pneumoniae* in pigs. The gene cluster has spread widely in the ecosystem, with various hosts identified. We speculate that *tmexCD1-toprJ1* initially proliferates in animals, particularly on chicken farms, before being transferred to humans through the food chain. Both clonal transmission and horizontal transmission contribute to its dissemination across ecological niches. Alarmingly, *tmexCD1-toprJ1* has reached broad-host-range plasmids and Hv-CRKP ST11-KL64 in healthcare settings, with most *tmexCD1-toprJ1*-positive Enterobacterales exhibiting resistance to nearly all antimicrobials, posing a significant threat to public health. Fortunately, due to the fitness cost associated with *tmexCD1-toprJ1*, the incidence of *tmexCD1-toprJ1*-positive Enterobacterales in food animals and humans has declined following the implementation of policies to restrict the use of antimicrobials in animal feed in China. This emphasizes that controlling sources and reducing antibiotic usage in food animals are effective strategies to combat antibiotic resistance. Given the substantial threat posed by MDR *tmexCD1-toprJ1*-positive *K. pneumoniae* to healthcare settings, close monitoring of *tmexCD1-toprJ1* across different ecological niches, particularly among poultry-origin *K. pneumoniae*, is necessary.

Availability of data and materials

Genome sequence data reported in this paper have been submitted to the NCBI database under the BioProject accession number: PRJNA1160055 (long-read data), and PRJNA1156631 (short-read data and long-read data).

CRediT authorship contribution statement

Luchao Lv: Software, Writing – review & editing, Writing – original draft, Visualization, Methodology, Formal analysis, Data curation. **Xun Gao:** Writing – review & editing, Investigation. **Chengzhen Wang:** Writing – review & editing, Writing – original draft. **Guolong Gao:** Software, Methodology. **Jie Yang:** Formal analysis. **Miao Wan:** Investigation. **Zhongpeng Cai:** Investigation. **Sheng Chen:** Writing – review & editing. **Jing Wang:** Investigation. **Chuying Liang:** Formal analysis. **Chao Yue:** Investigation. **Litao Lu:** Investigation. **Zhiyong Zong:** Writing – review & editing, Methodology, Investigation. **Jian-Hua Liu:** Supervision, Project administration, Methodology, Funding acquisition, Writing – review & editing, Writing – original draft, Visualization, Formal analysis, Conceptualization.

Declaration of competing interest

The authors declare that they have no known competing financial interests or personal relationships that could have appeared to influence the work reported in this paper.

Acknowledgments

This work was funded by the Guangdong Major Project of Basic and Applied Basic Research (2020B0301030007), the National Natural Science Foundation of China (32141002), the National Key Research and Development Program of China (2022YFC2303900), and the Science and Technology Program of Guangzhou, China (2023A04J0755 and 202201010300). We thank LetPub for its linguistic assistance during the preparation of this manuscript.

Appendix A. Supplementary data

Supplementary data to this article can be found online at https://doi.org/10.1016/j.eng.2025.03.038.

References

[1] World Health Organization (WHO). Who bacterial priority pathogens list. Report. Geneva: World Health Organization (WHO); 2024 May.
[2] Wang M, Earley M, Chen L, Hanson BM, Yu Y, Liu Z, et al. Clinical outcomes and bacterial characteristics of carbapenem-resistant *Klebsiella pneumoniae* complex among patients from different global regions (CRACKLE-2): a prospective, multicentre, cohort study. Lancet Infect Dis 2022;22(3):401–12.
[3] Wyres KL, Lam MMC, Holt KE. Population genomics of *Klebsiella pneumoniae*. Nat Rev Microbiol 2020;18(6):344–59.
[4] Agyeman AA, Bergen PJ, Rao GG, Nation RL, Landersdorfer CB. A systematic review and meta-analysis of treatment outcomes following antibiotic therapy among patients with carbapenem-resistant *Klebsiella pneumoniae* infections. Int J Antimicrob Agents 2020;55(1):105833.
[5] Lou T, Du X, Zhang P, Shi Q, Han X, Lan P, et al. Risk factors for infection and mortality caused by carbapenem-resistant *Klebsiella pneumoniae*: a large multicentre case-control and cohort study. J Infect 2022;84(5):637–47.
[6] Xiao T, Zhu Y, Zhang S, Wang Y, Shen P, Zhou Y, et al. A retrospective analysis of risk factors and outcomes of carbapenem-resistant *Klebsiella pneumoniae* bacteremia in nontransplant patients. J Infect Dis 2020;221(Suppl 2):S174–83.
[7] He T, Wang R, Liu D, Walsh TR, Zhang R, Lv Y, et al. Emergence of plasmid-mediated high-level tigecycline resistance genes in animals and humans. Nat Microbiol 2019;4(9):1450–6.
[8] Rodríguez-Baño J, Gutierrez-Gutierrez B, Machuca I, Pascual A. Treatment of infections caused by extended-spectrum-beta-lactamase-, AmpC-, and carbapenemase-producing *Enterobacteriaceae*. Clin Microbiol Rev 2018;31(2). e00079-17.
[9] Sun J, Chen C, Cui CY, Zhang Y, Liu X, Cui ZH, et al. Plasmid-encoded *tet*(X) genes that confer high-level tigecycline resistance in *Escherichia coli*. Nat Microbiol 2019;4(9):1457–64.
[10] World Health Organization (WHO). WHO publishes the WHO medically important antimicrobials list for human medicine [Internet]. Geneva: World Health Organization (WHO); 2024 Feb 8 [cited 2025 Mar 8]. Available from: https://www.who.int/news/item/08-02-2024-who-medically-important-antimicrobial-list-2024.
[11] World Health Organization (WHO). Aware classification of antibiotics for evaluation and monitoring of use [Internet]. Geneva: World Health Organization (WHO); 2023 Jul 26 [cited 2025 Mar 8]. Available from: https://www.who.int/publications/i/item/who-mhp-hps-eml-2023.04.
[12] Akiyama T, Presedo J, Khan AA. The *tetA* gene decreases tigecycline sensitivity of *Salmonella enterica* isolates. Int J Antimicrob Agents 2013;42(2):133–40.
[13] Beabout K, Hammerstrom TG, Perez AM, Magalhaes BF, Prater AG, Clements TP, et al. The ribosomal S10 protein is a general target for decreased tigecycline susceptibility. Antimicrob Agents Chemother 2015;59(9):5561–6.
[14] Moore IF, Hughes DW, Wright GD. Tigecycline is modified by the flavin-dependent monooxygenase *tet*X. Biochemistry 2005;44(35):11829–35.
[15] Sun Y, Cai Y, Liu X, Bai N, Liang B, Wang R. The emergence of clinical resistance to tigecycline. Int J Antimicrob Agents 2013;41(2):110–6.
[16] Lv L, Wan M, Wang C, Gao X, Yang Q, Partridge SR, et al. Emergence of a plasmid-encoded resistance-nodulation-division efflux pump conferring resistance to multiple drugs, including tigecycline, in *Klebsiella pneumoniae*. MBio 2020;11(2):e02930–e3019.
[17] Li Y, Sun X, Xiao X, Wang Z, Li R. Global distribution and genomic characteristics of *tet*(X)-positive *Escherichia coli* among humans, animals, and the environment. Sci Total Environ 2023;887:164148.
[18] Liu C, Guo J, Lu M, Shen N, Du P. Dissemination of the mobilised RND efflux pump gene cluster *tmexCD-toprJ* among *Klebsiella pneumoniae*. Lancet Microbe 2023;4(3):e135.
[19] Gao X, Wang C, Lv L, He X, Cai Z, He W, et al. Emergence of a novel plasmid-mediated tigecycline resistance gene cluster, *tmexCD4-toprJ4*, in *Klebsiella quasipneumoniae* and *Enterobacter roggenkampii*. Microbiol Spectr 2022;10(4). e001094-22.
[20] Wang CZ, Gao X, Liang XH, Lv LC, Lu LT, Yue C, et al. *Pseudomonas* acts as a reservoir of novel tigecycline resistance efflux pump *tmexC6D6-toprJ1b* and *tmexCD-toprJ* variants. Microbiol Spectr 2023;11(3):e00767–823.
[21] Wang CZ, Gao X, Yang QW, Lv LC, Wan M, Yang J, et al. A novel transferable resistance-nodulation-division pump gene cluster, *tmexCD2-toprJ2*, confers tigecycline resistance in *Raoultella ornithinolytica*. Antimicrob Agents Chemother 2021;65(4):e02229–320.
[22] Wang C, Gao X, Lv L, Cai Z, Yang J, Liu J. Novel tigecycline resistance gene cluster *tnfxb3-tmexCD3-toprJ1b* in *proteus* spp. and *Pseudomonas aeruginosa*, co-existing with *tet*(X6) on an SXT/R391 integrative and conjugative element. J Antimicrob Chemother 2021;76(12):3159–67.
[23] Wang J, Jiang Y, Lu MJ, Wang ZY, Jiao X. Emergence of a novel tigecycline resistance gene cluster *tmexC3-tmexD5-toprJ2b* in *oceanimonas* sp. from chicken, China. J Antimicrob Chemother 2023;78(5):1311–3.
[24] Hirabayashi A, Dao TD, Takemura T, Hasebe F, Trang LT, Thanh NH, et al. A transferable IncC-IncX3 hybrid plasmid cocarrying bla_{NDM-4}, *tet*(X), and *tmexCD3-toprJ3* confers resistance to carbapenem and tigecycline. MSphere 2021;6(4):e00592–621.
[25] Peng K, Li Y, Wang Q, Yang P, Wang Z, Li R. Integrative conjugative elements mediate the high prevalence of *tmexCD3-toprJ1b* in *proteus* spp. of animal source. mSystems 2023;8(5):e00429–523.
[26] Kim DW, Cha CJ. Antibiotic resistome from the one-health perspective: understanding and controlling antimicrobial resistance transmission. Exp Mol Med 2021;53(3):301–9.
[27] He W, Gao M, Lv L, Wang J, Cai Z, Bai Y, et al. Persistence and molecular epidemiology of bla_{NDM}-positive gram-negative bacteria in three broiler farms: a longitudinal study (2015–2021). J Hazard Mater 2023;446:130725.
[28] Peng K, Wang Q, Yin Y, Li Y, Liu Y, Wang M, et al. Plasmids shape the current prevalence of *tmexCD1-toprJ1* among *Klebsiella pneumoniae* in food production chains. mSystems 2021;6(5):e00702–21.
[29] Sun S, Gao H, Liu Y, Jin L, Wang R, Wang X, et al. Co-existence of a novel plasmid-mediated efflux pump with colistin resistance gene *mcr* in one plasmid confers transferable multidrug resistance in *Klebsiella pneumoniae*. Emerg Microbes Infect 2020;9(1):1102–13.
[30] Dong N, Zeng Y, Wang Y, Liu C, Lu J, Cai C, et al. Distribution and spread of the mobilised RND efflux pump gene cluster *tmexCD-toprJ* in clinical gram-negative bacteria: a molecular epidemiological study. Lancet Microbe 2022;3(11):e846–56.
[31] Sun L, Wang H, Meng N, Wang Z, Li G, Jiao X, et al. Distribution and spread of the mobilized RND efflux pump gene cluster *tmexCD-toprJ* in *Klebsiella pneumoniae* from different sources. Microbiol Spectr 2023;11(4):e05364–422.
[32] Yan Z, Wang P, Wang H, Zhang J, Zhang Y, Wu Y, et al. Emergence and genomic epidemiology of tigecycline resistant bacteria of fly origin across urban and rural China. Environ Int 2024;193:109099.
[33] CLSI M100: Performance standards for antimicrobial susceptibility testing, 31st edition. CLSI standard. Wayne: Clinical and Laboratory Standards Institute (CLSI); 2021.
[34] Yang J, Wu R, Xia Q, Yu J, Yi LX, Huang Y, et al. The evolution of infectious transmission promotes the persistence of *mcr-1* plasmids. MBio 2023;14(4): e00442–523.

[35] Machuca J, Briales A, Labrador G, Diaz-de-Alba P, Lopez-Rojas R, Docobo-Perez F, et al. Interplay between plasmid-mediated and chromosomal-mediated fluoroquinolone resistance and bacterial fitness in *Escherichia coli*. J Antimicrob Chemother 2014;69(12):3203–15.
[36] Bankevich A, Nurk S, Antipov D, Gurevich AA, Dvorkin M, Kulikov AS, et al. Spades: a new genome assembly algorithm and its applications to single-cell sequencing. J Comput Biol 2012;19(5):455–77.
[37] Wick RR, Judd LM, Gorrie CL, Holt KE. Unicycler: resolving bacterial genome assemblies from short and long sequencing reads. PLOS Comput Biol 2017;13(6):e1005595.
[38] Schwengers O, Jelonek L, Dieckmann MA, Beyvers S, Blom J, Goesmann A. Bakta: rapid and standardized annotation of bacterial genomes via alignment-free sequence identification. Microb Genom 2021;7(11):e000685.
[39] Lam M, Wick RR, Watts SC, Cerdeira LT, Wyres KL, Holt KE. A genomic surveillance framework and genotyping tool for *Klebsiella pneumoniae* and its related species complex. Nat Commun 2021;12(1):4188.
[40] Feldgarden M, Brover V, Gonzalez-Escalona N, Frye JG, Haendiges J, Haft DH, et al. AMRfinderplus and the reference gene catalog facilitate examination of the genomic links among antimicrobial resistance, stress response, and virulence. Sci Rep 2021;11(1):12728.
[41] Sullivan MJ, Petty NK, Beatson SA. Easyfig: a genome comparison visualizer. Bioinformatics 2011;27(7):1009–10.
[42] Treangen TJ, Ondov BD, Koren S, Phillippy AM. The harvest suite for rapid core-genome alignment and visualization of thousands of intraspecific microbial genomes. Genome Biol 2014;15(11):524.
[43] Tonkin-Hill G, Lees JA, Bentley SD, Frost S, Corander J. RhierBAPS: an R implementation of the population clustering algorithm hierBAPS. Wellcome Open Res 2018;3:93.
[44] Letunic I, Bork P. Interactive Tree of Life (iTOL) v5: an online tool for phylogenetic tree display and annotation. Nucleic Acids Res 2021;49(W1):W293–6.
[45] Idola D, Mori H, Nagata Y, Nonaka L, Yano H. Host range of strand-biased circularizing integrative elements: a new class of mobile DNA elements nesting in gammaproteobacteria. Mob DNA 2023;14(1):7.
[46] Wang X, Sun N, Liu X, Li F, Sun J, Huang J, et al. Small clone dissemination of *tmexCD1-toprJ1*-carrying *Klebsiella pneumoniae* isolates in a chicken farm. J Glob Antimicrob Resist 2022;29:105–12.
[47] Hirabayashi A, Yano H, Yahara K, Aoki S, Sugawara Y, Kajihara T, et al. Emergence of the mobile RND-type efflux pump gene cluster *tmexCD1-toprJ1* in *Klebsiella pneumoniae* clinical isolates in Japan. J Antimicrob Chemother 2025;80(1):192–9.
[48] Hirabayashi A, Ha V, Nguyen AV, Nguyen ST, Shibayama K, Suzuki M. Emergence of a plasmid-borne tigecycline resistance in *Klebsiella pneumoniae* in Vietnam. J Med Microbiol 2021;70(3):001320.
[49] Gao X, Yue C, Gao Y, Lu L, Liu JH, Lv L. Plasmid-mediated tigecycline resistance gene cluster *tmexCD1-toprJ1* emerged in *Klebsiella pneumoniae* from weever (*Lateolabrax maculatus*). Int J Antimicrob Agents 2024;64(6):107368.
[50] Liu Y, Gao X, He X, Lv L, Jiao Y, Yu R, et al. Emergence of the tigecycline resistance gene cluster *tmexCD1-toprJ1* in an IncC plasmid and citrobacter portucalensis. J Antimicrob Chemother 2022;77(7):2030–3.
[51] Sun S, Wang Q, Jin L, Guo Y, Yin Y, Wang R, et al. Identification of multiple transfer units and novel subtypes of *tmexCD-toprJ* gene clusters in clinical carbapenem-resistant *Enterobacter cloacae* and *Klebsiella oxytoca*. J Antimicrob Chemother 2022;77(3):625–32.
[52] Wu Y, Zhuang Y, Wu C, Jia H, He F, Ruan Z. Global emergence of Gram-negative bacteria carrying the mobilised RND-type efflux pump gene cluster *tmexCD-toprJ* variants. Lancet Microbe 2024;5(2):e105.
[53] Liu Y, Zhou Q, He W, Lin Q, Yang J, Liu J. *mcr-1* and plasmid prevalence in *Escherichia coli* from livestock. Lancet Infect Dis 2020;20(10):1126.
[54] Wang Y, Xu C, Zhang R, Chen Y, Shen Y, Hu F, et al. Changes in colistin resistance and *mcr-1* abundance in *Escherichia coli* of animal and human origins following the ban of colistin-positive additives in China: an epidemiological comparative study. Lancet Infect Dis 2020;20(10):1161–71.
[55] Ling Z, Yin W, Shen Z, Wang Y, Shen J, Walsh TR. Epidemiology of mobile colistin resistance genes *mcr-1* to *mcr-9*. J Antimicrob Chemother 2020;75(11):3087–95.
[56] Wang X, Wang Y, Zhou Y, Li J, Yin W, Wang S, et al. Emergence of a novel mobile colistin resistance gene, *mcr-8*, in NDM-producing *Klebsiella pneumoniae*. Emerg Microbes Infect 2018;7(1):1–9.
[57] Bender RG, Sirota SB, Swetschinski LR, Dominguez RMV, Novotney A, Wool EE, et al. Global, regional, and national incidence and mortality burden of non-COVID-19 lower respiratory infections and aetiologies, 1990–2021: a systematic analysis from the global burden of disease study 2021. Lancet Infect Dis 2024;24(9):974–1002.
[58] Murray CJL, Ikuta KS, Sharara F, Swetschinski L, Robles Aguilar G, Gray A, et al. Global burden of bacterial antimicrobial resistance in 2019: a systematic analysis. Lancet 2022;399(10325):629–55.
[59] Yan S, Sun Z, Yang Y, Zhu D, Chen Z, Hu F, et al. Changing antimicrobial resistance profile of *Enterobacter* spp. isolates in hospitals across China: a seven-year analysis from the CHINET antimicrobial resistance surveillance program (2015–2021). One Health Advances 2024;2(1):11.
[60] Liu C, Du P, Yang P, Zheng J, Yi J, Lu M, et al. Emergence and inter- and intrahost evolution of pandrug-resistant *Klebsiella pneumoniae* coharboring *tmexCD1-toprJ1*, bla_{NDM-1}, and bla_{KPC-2}. Microbiol Spectr 2023;11(2):e02786–822.
[61] Xiao T, Peng K, Chen Q, Hou X, Huang W, Lv H, et al. Coexistence of *tmexCD-toprJ*, bla_{NDM-1}, and bla_{IMP-4} in one plasmid carried by clinical *Klebsiella* spp. Microbiol Spectr 2022;10(3):e00549–622.
[62] Yu Z, Gunn L, Wall P, Fanning S. Antimicrobial resistance and its association with tolerance to heavy metals in agriculture production. Food Microbiol 2017;64:23–32.
[63] Ikhimiukor OO, Odih EE, Donado-Godoy P, Okeke IN. A bottom-up view of antimicrobial resistance transmission in developing countries. Nat Microbiol 2022;7(6):757–65.
[64] Fu B, Xu J, Yin D, Sun C, Liu D, Zhai W, et al. Transmission of bla_{NDM} in Enterobacteriaceae among animals, food and human. Emerg Microbes Infect 2024;13(1):2337678.
[65] Zhai R, Fu B, Shi X, Sun C, Liu Z, Wang S, et al. Contaminated in-house environment contributes to the persistence and transmission of NDM-producing bacteria in a Chinese poultry farm. Environ Int 2020;139:105715.
[66] Liu J, Du SX, Zhang JN, Liu SH, Zhou YY, Wang XR. Spreading of extended-spectrum beta-lactamase-producing *Escherichia coli* ST131 and *Klebsiella pneumoniae* ST11 in patients with pneumonia: a molecular epidemiological study. Chin Med J (Engl) 2019;132(16):1894–902.
[67] Gu D, Dong N, Zheng Z, Lin D, Huang M, Wang L, et al. A fatal outbreak of ST11 carbapenem-resistant hypervirulent *Klebsiella pneumoniae* in a Chinese hospital: a molecular epidemiological study. Lancet Infect Dis 2018;18(1):37–46.
[68] Wang Q, Wang R, Wang S, Zhang A, Duan Q, Sun S, et al. Expansion and transmission dynamics of high risk carbapenem-resistant *Klebsiella pneumoniae* subclones in China: an epidemiological, spatial, genomic analysis. Drug Resist Updat 2024;74:101083.
[69] Harmer CJ, Hall RM. IS*26*-mediated formation of transposons carrying antibiotic resistance genes. MSphere 2016;1(2). e00038-16.
[70] Wan M, Gao X, Lv L, Cai Z, Liu JH. IS*26* mediates the acquisition of tigecycline resistance gene cluster tmexCD1-toprJ1 by incHI1B-FIB plasmids in *Klebsiella pneumoniae* and *Klebsiella quasipneumoniae* from food market sewage. Antimicrob Agents Chemother 2021;65(3):e02178–220.
[71] Zhao Q, Jiang Z, Li T, Cheng M, Sun H, Cui M, et al. Current status and trends in antimicrobial use in food animals in China, 2018–2020. One Health Advances 2023;1(1):29.
[72] Liu JH, Liu YY, Shen YB, Yang J, Walsh TR, Wang Y, et al. Plasmid-mediated colistin-resistance genes: *mcr*. Trends Microbiol 2024;32(4):365–78.